



#### **OPEN ACCESS**

EDITED BY Marek Bryiak. Wrocław University of Technology, Poland

Natarajan Elangovan, Saveetha University, India Guillaume Hopsort, University of Amsterdam, Netherlands

Daniel T. Hallinan, ☑ dhallinan@eng.famu.fsu.edu

RECEIVED 18 August 2025 ACCEPTED 13 October 2025 PUBLISHED 05 November 2025

Kim K, Hallinan DT Jr. (2025) Charged polymer membrane processing and its impact on membrane separation. Front, Membr. Sci. Technol. 4:1688243. doi: 10.3389/frmst.2025.1688243

© 2025 Kim and Hallinan. This is an openaccess article distributed under the terms of the Creative Commons Attribution License (CC BY). The use, distribution or reproduction in other forums is permitted, provided the original author(s) and the copyright owner(s) are credited and that the original publication in this journal is cited, in accordance with accepted academic practice. No use, distribution or reproduction is permitted which does not comply with these terms.

# Charged polymer membrane processing and its impact on membrane separation

Kyoungmin Kim<sup>1,2</sup> and Daniel T. Hallinan Jr.<sup>1,2</sup>\*

<sup>1</sup>Department of Chemical and Biomedical Engineering, Florida A&M University—Florida State University (FAMU-FSU) College of Engineering, Tallahassee, FL, United States, <sup>2</sup>Aero-propulsion, Mechatronics and Energy (AME) Center, Florida A&M University-Florida State University (FAMU-FSU) College of Engineering, Tallahassee, FL, United States

This review focuses on charged polymer membranes motivated by their growing importance in membrane-based separation technologies. Charged polymers have a long history in ion exchange chromatography, and thus charged polymer membranes are commonly termed ion-exchange membranes (IEMs). IEMs can be used in energy-efficient reverse osmosis desalination and are being studied for recovering valuable minerals from aqueous waste streams. Types of IEMs are first introduced, categorized by charge type, charge distribution and porosity. Synthesis of charged polymers is briefly discussed. Considerable attention is given to important membrane properties and methods for characterizing them. These properties include ion-exchange capacity (IEC), water content, structure, ionic conductivity, permeability, selectivity, and thermal and mechanical properties. A key challenge in membrane design is achieving high IEC, which is desired for high IEM selectivity. This is a challenge due to the high water uptake that accompanies high IEC. Relevant aspects of membrane structure include percolated ion channels, porous morphology and inert mechanical reinforcement phases. Membrane structure is essential in addressing the challenge of achieving high IEC and optimizing membrane performance. Structure is predominantly dictated by membrane processing. Thus, membrane processing methods, their benefits and drawbacks and their impact on structure are described in detail. These methods include solution casting, the paste method, extrusion, electrospinning, phase inversion, and an emerging method to form a composite IEM. Finally, specific IEM applications are discussed that hold great promise for circular economies. These applications include lithium extraction from battery waste, mining of desalination brine, and mineral recovery from semiconductor waste. A major driver for the growing interest in these applications is the demonstrated cost-effectiveness of membranes in commercial desalination. With on-going research advances, such success is probable in these extraction and recovery applications.

ion-exchange membrane, transport, separation, solution casting, paste method, extrusion, electrospinning, phase inversion

# 1 Introduction - membrane technology

The development of sustainable resources is one of the key global challenges to prevent the depletion of finite subterranean resources, alleviate environmental pollution, and mitigate climate change (Lenkiewicz, 2024; Garcia-Gutierrez et al., 2023). While numerous studies are being conducted in both industry and academia, particularly focusing on the advancement of renewable energy technologies and energy storage systems, resource recovery from industrial waste is also gaining significant attention, given its potential for economic value (Cath et al., 2021). Common recovery methods include precipitation, evaporation, and pyrolysis; however, membrane-based separation technologies are well-aligned with sustainability goals owing to their low energy consumption and operating cost (Sharkh et al., 2022; Panayotova and Panayotov, 2021).

Charged polymer membranes are commonly utilized across a range of industrial applications, including water treatment/ desalination (Kitto and Kamcev, 2023; Geise et al., 2014b; Werber et al., 2016b), mineral harvesting (Sharkh et al., 2022), biomedical products (Oh et al., 2019; Chen et al., 2016), energy conversion/storage (Hallinan and Balsara, 2013; Ramon et al., 2011; Doan et al., 2015), and chemical processing (Jaroszek and Dydo, 2016), thanks to their unique ion transfer and separation abilities. Unlike neutral polymer membranes, the processing of charged polymer membranes poses challenges due to the interactions between the charged species and due to the more complex syntheses involved in creating charged polymers (Ran et al., 2017; Tang et al., 2014). Therefore, selecting the right manufacturing technology is crucial to achieve uniformly controlled charge density, improved physical and chemical stability, increased uniform mechanical strength, membrane thickness.

Membrane separation performance, first and foremost, relies on the ability of a membrane to transport desired species while blocking undesired ones. Material/membrane properties such as charge density, thickness uniformity, chemical stability, and mechanical strength are crucial in determining the membrane transport properties. For charged membranes, not only is charge density important, but also the charge distribution offers ion transport pathways and governs the absorption of water and ions (Geise et al., 2014b; Voigt et al., 2002). Improved uniformity of the membrane thickness facilitates surface modification and enhances the thermomechanical properties by evenly distributing thermal and physical stress across the membrane, increasing its durability (Tsou et al., 1992; Oh et al., 2004; Cakmak and Simhambhatla, 1995). Enhanced surface smoothness enables efficient and consistent surface treatment to address fouling, contamination, and wetting issues (Khoiruddin et al., 2017; Sagle et al., 2009). With enhanced durability, the membranes can be used in many challenging environments such as high-voltage cathodes, high- or lowtemperature separation processes or the treatment of highly concentrated waste solvents, where high electrochemical, thermal, or mechanical stress is applied (Tanaka et al., 2010; Tanaka et al., 2011). Membrane thickness and surface uniformity are controlled by the manufacturing processes, which thus play an important role in enhancing transport, membrane longevity, and versatility of these membranes.

Bulk physical properties of polymer membranes are also important players in designing membranes with selective transport capability. Bulk physical properties are primarily determined by the chemical composition, the chain architecture, and any micro- to meso-structures that are present. Processing plays a significant role, in particular due to its effect on micro- and mesostructures (Kim K. et al., 2023). For example, nanophase separation of subsections of a charged polymer can occur, in particular charged and polar components separate from inert portions of the polymer. The solvent quality in solution-casting-based membrane processing, largely dictates the nanostructure that forms (Lee et al., 2011; Slade et al., 2010). Another example of how processing affects structure is in polymer blend membranes. In partially miscible polymers the phase-separated structure strongly depends on processing conditions that can trap the membrane in out-of-equilibrium states that affect the thermal stability and mechanical properties (Nguyen et al., 2022; Hosseini et al., 2012; Kim K. et al., 2023). Membrane extrusion is another example in which the processing conditions such as the screw design or screw configuration, barrel temperature, flow rate, post-extrusion calendering, and roll-to-roll tension should be carefully controlled and optimized to reduce thickness variation, surface roughness, and avoid film failure and thermal degradation (Giles et al., 2004).

The processing method should be carefully selected, considering the purposes and demands of the membranes as well as the characteristics and properties of the materials. Understanding the functionality of the charged polymers, capabilities and limitations of conventional processing technologies and the requirements from the industry will pave the way for design and development of optimal membrane processing while providing reduced cost and environmental impact. However, research in processing techniques focusing on charged membranes are limited and have not been thoroughly reviewed. The manufacturing processes have only been addressed in subchapters in a few reviews (Kusoglu and Weber, 2017; Xu, 2005; Ran et al., 2017). The reviews on preparation of charged polymer membranes are focused primarily on the synthesis techniques (Depuydt and Van der Bruggen, 2024; Nagarale et al., 2006; Ryoo et al., 2024). In this review, we explore the various processing technologies such as solution casting, paste method, extrusion, electrospinning and phase inversion, involved in the production of charged polymer membranes. The unique aspects, applications, capabilities and limitations of several polymer membrane processing technologies are discussed in detail. We also present an overview of membrane properties and characterization, emphasizing ion transport, permeability, and selectivity. Additionally, we discuss the feasibility of charged polymer membranes in practical applications in energy and sustainability sectors, specifically for recovery of materials from battery and desalination waste.

# 2 Charged polymer membranes

There is a long history of using charged polymer networks as ion-exchange resins, for example, in ion chromatography. Charged polymers have expanded into membrane formats, that are used in fuel cells, flow batteries and other battery types, surface coatings, and reverse-osmosis desalination. More recently, charged polymer

membranes have been identified as playing a crucial role in extracting valuable materials from battery and other mineral wastes. Cationic and anionic membranes, which selectively absorb or block specific charges, enable the separation of various ionic components. Membrane-based methods, such as nanofiltration and electrodialysis (ED), are of interest for extracting valuable minerals, such as bromine, magnesium, and lithium, from concentrated desalination brines (Aghaei et al., 2024; Sharkh et al., 2022). Membranes play an important role in concentrating brines in target ions, e.g., via nanofiltration, but IEMs require further development before electrodialysis and other membrane-based methods are ready for commercialization. These methods could potentially also be used to extract lithium and other valuable elements from battery waste (Hyder et al., 2025; Wamble et al., 2022).

# 2.1 Types of charged polymer membranes

We define IEMs as non-porous polymer films that contain ionic functional groups. Their ionic conductivity, hydrophilicity, and immobilized charge carriers make them suitable for a wide range of applications. Since the first synthetic ion-exchange resin was reported by Adams and Holmes (1935), extensive research has been conducted on the synthesis methods of IEMs, theoretical explanations of membrane phenomena, and their industrial applications.

IEMs can be classified based on the type of fixed ion-exchange groups: cation-exchange membranes (CEMs), anion-exchange membranes (AEMs), and amphoteric membranes. In addition, advanced processing techniques can be used to form bipolar membranes, charge mosaic membranes, and porous polymer membranes from IEM building blocks. CEMs possess negatively charged functional groups, allowing the selective transport of cations through the membrane. The functional groups in CEMs typically include sulfonate/sulfonic acid (most common), carboxylic acid, phosphonic acid, phosphoric acid ester, and various sulfonamides/ sulfonimides (common in polymer electrolytes for batteries). Various backbone chemistries have also been examined, with the most common being crosslinked styrene copolymers, poly(ether ether ketones) (PEEK), polysulfone (PSf)/poly(ether sulfone) (PES), and modified polyethylene (PE). Specific examples of chargebackbone combinations include sulfonated styrene-based derivatives (Safronova et al., 2016; Galizia et al., 2017), carboxylic acid installed on PE, polynorbornene, or PEEK via grafting or sidechain functionalization (Wang et al., 2017; Yang et al., 2024; Choi et al., 2000), phosphonic acid functionalized styrene derivatives (Sata et al., 1996), sulfonic acid functionalized hyperbranched PES (Kakimoto et al., 2010), mono- and di-phosphoric acid ester functionalized styrene derivatives (Selzer and Howery, 1986), perfluorinated polymers with sulfonic and carboxylic acid groups (Kirsh et al., 1990), sulfonamide functionalized acrylic acid-based polymer (Kojima et al., 1995), as well as commercially available membranes, such as Nafion, Aquivion, Fumasep, and Neosepta (Nagarale et al., 2006; Yee et al., 2012). AEMs contain positively charged functional groups, permitting the selective transport of anions. AEMs incorporate functional groups such as primary, secondary, and tertiary amines (Komkova et al., 2004), quaternary ammonium (Pham et al., 2017; Dekel et al., 2017), tertiary sulfonium (Lindenbaum et al., 1958), quaternary phosphonium (Kumari et al., 2021), cobaltocenium (Lin et al., 2023), and other positively charged moieties in aqueous or mixed aqueous-organic solvents, including complexes of alkali metals with crown ethers (Chen et al., 2023; Yang et al., 2021; Ryoo et al., 2024; Shaik et al., 2024). In commercial IEMs, sulfonic acid and carboxylic acid groups are most commonly used as cation-exchange groups, while quaternary ammonium groups are typically used as anion-exchange groups (Shaik et al., 2024; Henkensmeier et al., 2021).

Amphoteric IEMs have both cationic and anionic exchange groups distributed throughout the membrane. Bipolar IEMs consist of a bilayer structure composed of a cation-exchange layer and an anion-exchange layer. Charge mosaic membranes have domains of cationic and anionic exchange groups coexisting in the cross-sectional area of the membrane, often surrounded by insulating materials. Porous membranes are an effective strategy to increase permeability and flux in applications where this is of paramount importance.

# 2.1.1 Cation-exchange membranes

Adams and Holmes first synthesized a synthetic ion-exchange resin using the condensation polymerization of a formaldehydephenol complex (Adams and Holmes, 1935). Sulfonated phenol formaldehyde was chemically unstable due to the decomposition of C-H bonds caused by the formation of hydroperoxide radicals. Nafion is the first commercialized ion-exchange polymer membrane consisting of fluorinated backbone and sulfonic acid functional group (Mauritz and Moore, 2004). Nafion is a branched perfluorosulfonic acid (PFSA) polymer in which sulfonic acid groups are covalently bonded to fluorine-substituted alkyl ether side chains, with a backbone resembling the structure of Teflon. Because the acidic groups are covalently bound to the polymer backbone, there is no risk of the ion-conducting sites being leached from the membrane. Nafion exhibits exceptional ionic conductivity due to the high mobility of protons that are dissociated by water from sulfonate groups located at the end of flexible, saturated side chains. Due to its excellent ionic conductivity, chemical stability, and ion selectivity, PFSAs are widely used in fuel cells, seawater-based NaOH production, and electrodialysis of oxidizing solutions (Banerjee and Curtin, 2004).

Although PFSAs exhibit excellent ionic conductivity, chemical stability, and anion rejection, they face challenges such as high cost and poor selectivity, e.g., methanol and ion crossover are problems in direct methanol fuel cells and flow batteries, respectively (Hallinan and Elabd, 2007; Doan et al., 2015). To address these issues, hydrocarbon-based polymers are being developed as potential alternatives. Polymer membranes with various types of aromatic main chains, that can be sulfonated, have been attempted to improve chemical stability. Polyimide, PSf, and poly(ether ketone) (PEK) are gaining attention for their stability against strong acids and redox agents (Nagarale et al., 2006). Polyimide has excellent thermal stability, but its sensitivity to hydrolysis reaction is a drawback. For PEK and PEEK, a disadvantage is that the ketone group is reduced or forms an unstable benzyl group by active radicals generated from hydrogen peroxide at platinum catalyst (used in fuel cells) (Karimi et al., 2020; Vogel et al., 2010). PES is an amorphous polymer with a diphenyl sulfone,

diphenyl ether, and aromatic isopropylene structure, and has flexible chain, excellent thermal and mechanical properties, as well as high resistance to hydrolysis and hydrogenation reactivity (Zhao et al., 2013). The limitation of using PES in fuel cells is its low proton conductivity (Shah et al., 2024).

#### 2.1.2 Anion-exchange membranes

The most common use of AEMs is in fuel cells and water electrolysis, but unlike CEMs, far fewer have been commercialized largely due to challenges associated with the instability of cationic functional groups. Strongly basic environments occur in AEM fuel cells, that require exceptional chemical stability offered by fluorination, but fully fluorinated AEMs have not yet been commercialized due to synthetic challenges (Gottesfeld et al., 2018). Most of the fluorinated AEMs reported so far are hydrocarbon-based polymers in which fluorine is partially substituted. An example of a fully fluorinated AEM is a polymer built from decafluorobiphenyl and 4,4'-(hexafluoroisopropylene) diphenol, which showed high ionic conductivity and excellent mechanical strength and chemical stability (Gao et al., 2020).

Quaternary ammonium is commonly used as the cationic group in AEMs. Operational lifetime is limited primarily by degradation of quaternary ammonium. The quaternary ammonium ions are prone to degradation under alkaline conditions by competing mechanisms of Hofmann elimination (E2) and bimolecular nucleophilic substitution (SN2) (Bauer et al., 1990). E2 is dominant when the sidechain has two or more carbons between the polymer backbone and the quaternary ammonium. Transformation of the quaternary ammonium group to tertiary amine through ylide intermediates is another degradation mechanism of cationic polymers (Espiritu et al., 2018). Heterogeneous membranes of alkyl/aryl blends or copolymers can provide steric hindrance to reduce the exposure of the quaternized ammonium to hydroxide ions (OH-) (Bauer et al., 1990). Marino et al. showed that the chain length and ring architecture of side chains play an important role to prevent the attack of hydroxide ions (Marino and Kreuer, 2015). Ether-free polymers can enhance the alkaline stability due to the absence of ether groups that are weak to hydrolysis and chain scission (Hu et al., 2025; Sankar et al., 2023). The alkaline stability was found to be highly dependent on the chemical nature of the R groups in the quaternary ammonium cations due to their effect on degradation mechanisms (Ye et al., 2013; Arges et al., 2012).

Since the improvement of alkaline stability typically includes significant modifications of material design, selecting an appropriate processing method for an AEM may rely on the specific mitigation strategy employed. The properties of reinforced AEMs with etherfree architecture, alkyl-aryl spacing or stable cation groups can largely impact the processability of the membranes. For example, ether-free polymers and polyarylene-containing membranes typically have higher modulus but lower flexibility and solubility in polar solvents. These materials can require higher processing temperatures for melt processing and can have limited solvent selection for solution casting. The miscibility of polymer blends and the thermal properties of the materials with different cation groups should also be considered when selecting the processing methods for AEMs.

Hydrocarbon-based AEMs can be categorized into two main groups: ether-containing and ether-free polymers (Shaik et al.,

2024). Ether-containing AEMs include poly(arylene ether ketone) bearing cyclic ammonium or imidazolium groups, poly(2,6-dimethyl-1,4-phenylene oxide) with aliphatic cationic side chains, and quaternary ammonium-functionalized PSf. These ether-containing AEMs suffer from high production cost and poor long-term durability due to degradation of both the ether groups in the polymer backbone and the cationic groups (Parrondo et al., 2014; Ryoo et al., 2024).

Ether-free AEMs are generally divided into polyethylene-based and polyarylene-based AEMs. Polyethylene-based AEMs are composed of C–C bonds in backbones with high number-average molecular weights. Zhang et al. synthesized polyethylene-based AEMs functionalized with ammonium chloride groups, with or without crosslinking (Zhang et al., 2011). The crosslinked membranes exhibited excellent tensile modulus (273 MPa) and strength (20 MPa) and high ionic conductivities in HCl and CuCl<sub>2</sub> solutions at room temperature.

Polyarylene-based AEMs are ether-free membranes with aromatic ring backbones. A high-performing polyarylene-based AEM example was developed by Soni et al., based on poly(fluorene-alt-tetrafluorophenylene) functionalized aromatic trimethylammonium groups. It exhibited a high performance for alkaline water electrolysis, high OHconductivity, and excellent durability (Soni et al., 2020). Chen et al. reported the development of a poly(fluorenyl-co-aryl piperidinium) (PFAP)-based anhydrous anodic AEM water electrolyzer. The system achieved a high current density of 7.68 A/cm<sup>2</sup> at 2.0 V and 80 °C, with excellent water diffusivity  $(9.38 \times 10^{-8} \text{ cm}^2/\text{s})$  and ionic conductivity (160 mS/cm at 80 °C). It also demonstrated outstanding durability, maintaining a stable voltage of 0.5 V for 1,000 h at 60 °C under a current density of 0.5 A/cm<sup>2</sup> (Chen et al., 2021).

In a rare study of separation with AEMs, Bryjak et al. examined Boron separation (Bryjak et al., 2007). Boron permeation through an AEM was driven by the Donnan potential between a concentrated feed slurry containing a Boron-selective resin and a dilute receiving solution. This Donnan dialysis was able to regenerate the Boron selective resin and demonstrates that AEMs may also hold potential for mineral harvesting via membrane separation.

# 2.1.3 Amphoteric polymers

Amphoteric polymers are another class of IEMs that are functionalized with both positively and negatively charged groups. Amphoteric polymers contain a uniform distribution of cationic and anionic functional groups, which distinguishes them from charge mosaic membranes, in which cationic and anionic functionalities are relegated to separate nanostructured regions. Amphoteric IEMs have been used as separators in Vanadium redox flow batteries (Liu et al., 2021). Amphoteric IEMs have been synthesized by modifying commercial AEMs with cationexchange polymer, either via surface modification or by incorporation into crosslinking moieties, and evaluated in permselective electrodialysis (Liao et al., 2019). Zwitterionic IEMs (ZwIEMs) are a specific subset of amphoteric IEMs. A zwitterionic functional group contains both a cation and an anion. Thus, the cationic and anionic functionalities are collocated in ZwIEMs. Zwitterions are widely used to modify the surface of membranes by treating the surface of the base membrane with grafting or dip

coating a substance with a zwitterionic functional group such as phosphobetaine, carboxylbetaine, and sulfobetaine in which quaternary ammonium and acid are bound to the polymer. The pH at which the surface charge of ZwIEM becomes zero is called the isoelectric point, where both positive and negative ionic species are prevented from binding to the surface. The surface modification prevents membrane fouling and improves performance (Schlenoff, 2014). It can also be applied to ion-exchange resins (Ghoussoub et al., 2018).

#### 2.1.4 Bipolar membranes

Bipolar membranes are IEMs that integrate cation-exchange layers and anion-exchange layers in a single structure. These membranes have various structures depending on their applications. The cation-exchange layer can pass hydrogen ions and the anion-exchange layer can pass hydroxyl ions. To produce acids and bases from aqueous salt solutions, electrodialysis can be used to decompose water at the contact surface of the bipolar membrane. In adjacent liquid chambers, the H<sup>+</sup> and OH<sup>-</sup> from water decomposition combine with anions and cations from salt forming acids and bases, respectively (Kovalev et al., 2022; Mazrou et al., 1998). In the energy conversion process, the neutralization of protons and hydroxide ions at the bipolar membrane interface induces a potential difference generating electrical energy and assisting in fuel cell hydration (Daud et al., 2022). While bipolar membrane fuel cells are a new research area, their use in electrodialysis-based systems is more developed.

Bipolar membranes are fabricated by hot pressing a CEM and an AEM together with catalyst and polymer binder in between (Kovalev et al., 2022). Bipolar structure can also be formed by casting an anion-exchange solution on top of a CEM (or *vice versa*) after applying a catalyst, followed by drying. Grafting methods can be employed, in which ion-exchange groups are grafted onto the surface of a prepared membrane.

### 2.1.5 Porous IEMs

In general, IEMs possess nanoscale ion channels but no pores for fluid flow. Therefore, compared to porous membranes, IEMs have low water transmittance and high energy consumption. Porous IEMs are being investigated for ion-exchange processes where enhanced permeation rates are desired and high ionic selectivity is not a critical requirement. Kim et al. applied a porous IEM to a microbial fuel cell (MFC) (Kim et al., 2014). A porous membrane was fabricated via one-step phase inversion method using poly(vinylidene fluoride) (PVDF). The pores were activated through grafting reaction using benzoyl peroxide as an oxidizing agent and then sulfonated. The resulting membrane exhibited an average pore size of approximately 10 nm, and the proton transference number was 0.97. The membrane demonstrated excellent long-term performance in MFC operation.

There are a variety of approaches to synthesizing porous IEMs. One method involves ionic functionalization of polymers of intrinsic microporosity (PIMs) (Li et al., 2025). PIMs contain a significant amount of free volume due to steric constraints in their chemical design that endow them with three-dimensional porous structures and increased specific surface area. These features can be leveraged to facilitate gas release or absorption at the surface of electrodes or capacitors. The application of PIMs has expanded from early use in

gas separation to batteries, fuel cells and flow batteries, driven by advances in the precise control of pore architecture and the incorporation of ion-conducting functionality.

More conventional methods of forming porous polymer membranes include 1) attaching ion-exchange groups to a porous support membrane, 2) electrospinning ion-exchange polymers, or 3) mixing ion-exchange polymer solution with a non-solvent to induce phase separation (non-solvent induced phase separation, NIPS). The porous support membrane requires sufficient pore size and porosity to allow infiltration of the ion-exchange polymer, and compatibility of the porous matrix and the ion-exchange polymer to prevent graft detachment or leaching of the functional groups during operation. In electrospinning, parameters such as nozzle size, solution concentration, and spinning speed determine the fiber diameter, pore size, and porosity. For NIPS, pore size and porosity can be controlled by the miscibility and concentration of the non-solvent (Bridge et al., 2022b). Both electrospinning and NIPS are discussed in detail in Section 4 Processing Techniques.

# 2.2 Synthesis of charged membranes

The synthesis methods of charged polymers have been extensively studied and reviewed (Nagarale et al., 2006; Depuydt and Van der Bruggen, 2024; Ryoo et al., 2024). Therefore, we will only briefly mention a few of the most important synthetic approaches. These include: 1) polymerization of charged monomers (Adams and Holmes, 1935; Vijayakrishna et al., 2008; Wiley and Reed, 1956), 2) functionalization of neutral polymers using, for example, amination or sulfonation (Alexandrova and Iordanov, 1995; Alexandrova and Iordanov, 2001; Yee et al., 2013; Gohil et al., 2006), and 3) grafting substrate polymer membranes with ionic groups (El-Rehim et al., 2000; Kim et al., 2014; Mokrini and Huneault, 2006).

The presence of ionic functionality makes the polymer hydrophilic, the degree of hydrophilicity increasing with charge density. Most applications of IEMs are in aqueous environment, which requires consideration of water uptake (to be discussed in detail below). Swelling due to water uptake can adversely affect membrane mechanical strength, which is problematic in purification or separation processes (Kamcev and Freeman, 2016). Swelling can be controlled via copolymerization and/or crosslinking (Nagarale et al., 2006). Preparation of crosslinked charged polymer membranes includes two main methods: one involves crosslinking ionized polymers directly (Brijmohan et al., 2005), while the other introduces functional groups into a crosslinked polymer substrate (Shahi et al., 2000). Composite or blend membranes can also be formed by mechanically mixing charged species with non-charged matrix to compensate the weakened mechanical properties of charged polymers in aqueous environments, see Section 4.2 Paste Method (Kim S. et al., 2023; Bulejko and Stránská, 2018).

Due to the plethora of routes for synthesizing charged polymers, one must first consider the thermal, physical, and chemical characteristics of the membrane that are required for the application of interest. For example, the ion-exchange functional group(s) should have chemical stability in the operating conditions of interest, such as under strong acid or strong base conditions.

Moreover, the choice of polymer repeat unit(s) will impact the maximum achievable IEC, which is inversely proportional to monomer molecular weight. For example, the IEC of fully sulfonated polystyrene (sPS) is 5.43 meq/g, whereas the bulkier repeat unit of sulfonated PEEK (sPEEK) is 2.72 meq/g. Of course, addition of neutral comonomers and/or crosslinking agents will further reduce the maximum achievable IEC, but are often necessary to prevent dissolution/swelling of the membrane as discussed above. Only after considering what is the appropriate chemistry to achieve thermal, mechanical, and chemical stability, can the best synthetic method be selected.

For the purposes of this review, we focus on the subsequent selection of the processing method (Section 4) that best complements the selected polymer chemistry to arrive at optimal performance properties. Important considerations in this regard include the effect of polymer chemistry on 1) its solvent solubility, 2) its softening temperature, and 3) its ability to flow. For example, ionization of a hydrophobic polymer dramatically affects its solubility, often requiring a transition from a hydrocarbon solvent to a polar solvent such as water. This positively impacts considerations such as volatile organic content. It also is likely to require the use of a solvent with lower volatility that will slow evaporation and thus membrane formation rate in solution-based processing. These tradeoffs should be considered when deciding whether to ionize before or after membrane formation. Another consideration is the molecular weight of the polymer, which strongly affects solution viscosity and thus how the solution spreads. Polymer chemistry design and membrane process engineering are coupled to the extent that they constrain each other. For example, approaches to control swelling, such as crosslinking, will also prevent flow, requiring that the membrane be formed prior to crosslinking.

# 2.3 Ion channels

Compared to neutral polymers, charged polymers exhibit significant dependence of physical properties on water content, which is strongly influenced by the nature and density of their ionic functional groups. The incorporation of charged groups imparts hydrophilicity to the polymer increasing both ionic conductivity and water solubility. By regulating the composition of hydrophobic and hydrophilic moieties, nanostructures can be achieved which consists of two distinct domains: a hydrophobic polymer backbone (or segment) and a hydrophilic phase with ionized functional groups. The hydrophobic components prevent dissolution in aqueous media and provide required membrane mechanical stability. Water molecules associate with the ionized groups to form hydrated ion clusters, which are segregated from the hydrophobic phase. These hydrated clusters are interconnected forming nanochannels which serve as continuous pathways for ion and water transport (Li et al., 2025).

The ion permeation and selectivity significantly depend on the dimensional factors of the ion channels: channel diameter  $(d_c)$  and Debye length  $(\lambda_D)$ . Debye length represents the effective thickness of electric double layers (EDL) developed in the vicinity of channel walls due to the attraction of counter-ions by the charged groups. When the channel diameter is smaller than the Debye length  $(d_c < \lambda_D)$ , the counter-ion transport is promoted while the co-ion is

rejected, resulting in increased selectivity. For dilute solutions in a homogeneous dielectric medium, the Debye length is determined by many factors such as dielectric constant of the solution  $(\epsilon_r)$ , temperature (T), concentration  $(c_i)$  and valence  $(z_i)$  of ionic species i as described in Equation 1 (Muthukumar, 2023; Li et al., 2025):

$$\lambda_D = \sqrt{\frac{\epsilon_r \epsilon_0 k_B T}{2N_A e^2 I}}, I \equiv \frac{1}{2} \sum_i z_i^2 c_i \tag{1}$$

where  $\epsilon_0$  is the dielectric constant of vacuum,  $k_B$  is Boltzmann constant, e is electron charge,  $c_i$  is in units of mol/m³ and I is the ionic strength. With increased IEC, increased water uptake expands the diameter of nanochannels and promotes ion permeation. On the other hand, increased IEC is expected to enhance Donnan exclusion by increasing membrane potential and excluding co-ions. Thus, co-ion transport is often observed to have a non-monotonic dependence on IEC, due to the competing effects of water promoting ion transport and fixed charged content promoting Donnan exclusion. Therefore, ion flux and selectivity inherently exhibit a trade-off relationship (Kitto and Kamcev, 2024). Many efforts have been attempted to overcome this limitation by increasing ion transport channels while suppressing swelling, through control of polymer architecture, formation of micropores, and modification of membrane surface (Mizutani, 1990).

Nafion exhibits an interesting nanostructured, percolated network, that can explain its high ionic conductivity with low water uptake, which is contrary to the general trend of ionic conductivity as a function of water content, as many other especially hydrocarbon IEMs exhibit. The high ionic conductivity of Nafion is explained by its well-organized cluster-channel network (Gierke and Hsu, 1982). Hsu and Gierke theoretically described the relationship between ionic cluster formation and ion transport phenomena in PFSA membranes through which estimation of cluster diameters was enabled based on key parameters such as water uptake, equivalent weight, and cation type (Hsu and Gierke, 1983). According to their percolation model, Nafion exhibited sharply increased conductivity over a critical hydration threshold. Interestingly, carboxylated fluorinated polymers showed higher Na<sup>+</sup> and Cs+ diffusion coefficients but lower water uptake than Nafion, due to more sharply defined ion channels (Yeager et al., 1982).

# 3 Membrane properties and characterization

As mentioned in the introduction, numerous material properties affect membrane characteristics. Here, we focus on membrane properties that determine suitability for salt and ion separation methods. Membrane charge density is a paramount consideration that is quantified by IEC. IEC largely dictates not only how well a membrane excludes co-ions, but also how much water it takes up. IEC is important because membranes used in water treatment processes, such as electrodialysis, must have a high selectivity in which cations or anions pass while co-ions are excluded (Werber et al., 2016a). The charged and hydrophilic nature of IEMs can lead to considerable swelling when they are exposed to aqueous environment. Swelling affects the membrane structure, which plays a significant role in transport properties (ionic

conductivity and permeability) and can weaken the membrane. It is important for a membrane to prevent mixing of the retentate and permeate streams in a separation process in which high flow rates and/or pressure gradients are often present. Thus, their mechanical integrity, even in the hydrated state, must be maintained, which requires that degree of swelling and mechanical properties are considered when designing them. Finally, thermal properties of the membrane are important for maintaining functionality at the operating temperature of the separation process. In this section, the properties that are required for water treatment and ion separation are discussed, as well as how the properties are characterized.

# 3.1 Ion-exchange capacity

Ion-exchange capacity is the millimoles of charge fixed to the membrane (often termed milliequivalents) per gram of dry membrane (meq/g<sub>dry</sub>). There are several ways to determine the IEC of an IEM. These include direct measurement of atomic composition, nuclear magnetic resonance spectroscopy (NMR), and ion-exchange followed by titration, which is the most common approach (Leo et al., 2024). For the titration approach in a CEM, the counter-ions associated with the polymer are exchanged with counter-ions from a salt or acid solution. If the membrane is in acid form salt should be used and if the membrane is in ionic form acid should be used so that the amount of protons released into or consumed from the solution can be measured with a pH-based titration. Similarly, the IEC of an AEM can be measured by exchanging the anions associated with cationic functional groups with counter-ions in a salt or alkaline solution and then titrating the final solution to determine change in OH-. AEM should not be used with strong base due to the low chemical stability of their functional groups under high-pH conditions. In addition, when titrating in air, carbonic acid that forms from dissolution of CO2 in water will partially neutralize the basic solution, causing error in the titration.

A more accurate IEC can be measured using NMR. The molar fraction of the ionized group can be calculated by comparing the peak areas of ionized and non-ionized groups (Equation 2). Dividing the fraction by the weighted sum of molecular weights of ionized and neutral functional groups yields the IEC,

IEC = 
$$\frac{x}{M_{neutral}(1-x) + M_{ionized}x}$$
 (2)

where x is the mole fraction of charged species, M is the molecular weight, and subscripts *neutral* and *ionized* represent neutral and ionized species, respectively.

### 3.2 Water content

The water content (WC) is an important parameter that affects the permselectivity and mechanical properties of IEMs. The WC of an IEM is measured gravimetrically as the ratio of water mass in the hydrated membrane  $(m_{wet} - m_{dry})$  to dry membrane mass  $(m_{dry})$ . The IEM is cut into an appropriate size and immersed in distilled water to reach an equilibrium state. Then, after removing surface water, the weight is measured. After drying the samples under

vacuum at elevated temperature and measuring the weight, the water content is calculated using Equation 3.

$$WC = \frac{m_{wet} - m_{dry}}{m_{dry}} \tag{3}$$

It is important to measure water content under the conditions in which the membrane will be used, because it is a function of the composition of the external solution. For this reason, it is common not only to measure WC when equilibrated with pure deionized water, but also in equilibrium with aqueous solutions, 1 mol/L salt in water being a commonly used condition. An osmotic pressure difference exists between the external solution and the membrane, and it is this that drives water sorption into the membrane, resisted primarily by the entropic penalty associated with stretching of the polymer chains that comprise the membrane (Flory, 1953). The moles of solutes in the external solution reduce the osmotic pressure, which is why WC should be measured under appropriate conditions. It is best practice to measure not only gravimetric but also volumetric sorption, as the swollen volume (or equivalently density) is needed to calculate molar concentration of fixed charges and of co-ions. Co-ion concentration in the membrane can play a major role in carrying ionic current and in permselectivity, discussed below. Co-ion concentration is most easily quantified with desorption measurements. After the equilibration in an aqueous solution and drying required for measuring WC, the membrane is placed in a known amount of pure water to draw sorbed co-ions (and their associated counter-ions that ensure electroneutrality) out of the membrane. The moles of desorbed co-ions is then measured to determine what had been the co-ion concentration in the membrane. The gold standard for this measurement is ion chromatography.

# 3.3 Structure

In the dry state, IEMs are dense materials that lack pores and ion channels. Nanometer-scale ion channels develop when IEMs are hydrated, and these channels enable the transport of ions. Ion channels are interconnected network structures with non-uniform diameter, typically of ~1-5 nm, containing water molecules, ions and other hydrophilic components of the polymer (Wang et al., 2021; Li et al., 2025). Ion channels act as electrolytes that absorb solutions and transfer ions along connected charged functional groups. Permeability and selectivity of the membranes are governed by structural factors such as the volume fraction of nanochannels that affect their connectivity and tortuosity. When charge density increases, the water volume fraction increases resulting in higher permeability of both water and ions. However, higher water volume fractions cause selectivity to decrease due to reduced membrane potential, and the physical integrity of the membrane can be compromised by extreme amounts of swelling. When a crosslinked IEM is formed, swelling due to water uptake is suppressed and the mechanical properties are reinforced, but permeability and flexibility decrease. Increased volume fraction of hydrophobic blocks in a block copolymer has a similar effect to increased crosslinking. Thus, the permeability, selectivity, and mechanical properties of IEMs can be balanced by controlling the degree of crosslinking or volume fraction of the hydrophobic phase.

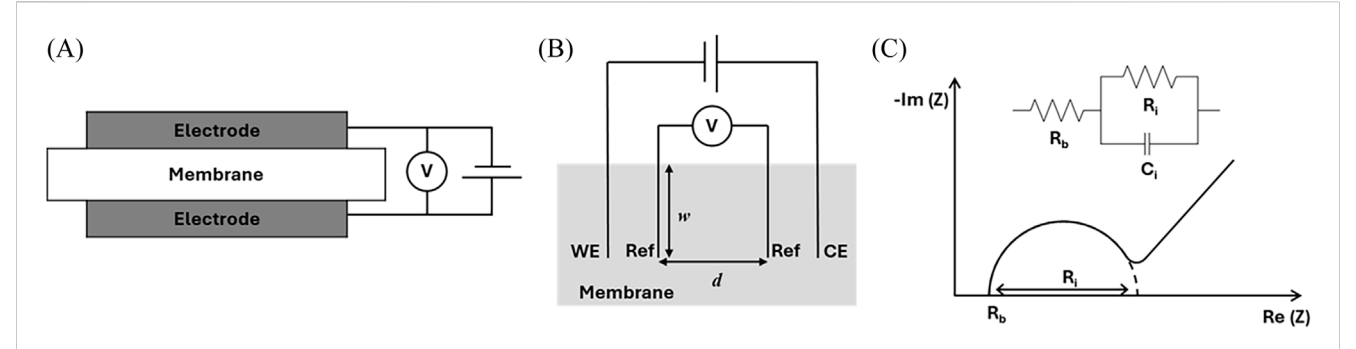


FIGURE 1

Schematics of setups for electrochemical impedance spectroscopy (EIS) of IEMs to measure ionic conductivity: (A) two-electrode format in which the current is carried by and voltage is measured between the same two electrodes and (B) four-electrode format with alternating current applied between the working electrode (WE) and the counter electrode (CE) and alternating voltage measured between the two reference (Ref) electrodes. Due to the alternating nature of the measurement, it is also possible to conduct EIS by applying voltage and measuring current, in either format. (C) Schematic of a Nyquist plot representation of the complex impedance from an EIS measurement that extends from high frequency on the left-hand side of the figure to a low-frequency diffusive tail on the right-hand side of the figure. An equivalent circuit is shown in the inset for the high-frequency data that includes a resistor representing bulk membrane resistance ( $R_b$ ) and a parallel combination of interfacial resistance ( $R_i$ ) and capacitance ( $R_i$ ) associated with the electrode-electrolyte interfaces. Theoretical impedance from this equivalent circuit is shown as a dashed semicircle that overlaps the high-frequency portion of the data (solid curve).

The hierarchical structure of nanophase-separated IEMs can be characterized by transmission electron microscopy (TEM), atomic force microscopy (AFM), wide-angle x-ray scattering (WAXS), smallangle x-ray scattering (SAXS), and small-angle neutron scattering (SANS) (Gao et al., 2020; Baird et al., 2025; Hensley and Way, 2007; Chan et al., 2020; Gebel and Diat, 2005). TEM is a powerful tool to directly visualize the size, shape and distribution of ion clusters through the membranes, but has limitations of ultrathin sample size (<100 nm) and weak contrast due to the low atomic numbers of elements in the polymers (Xue et al., 1989). Surface images of the membranes can be achieved by AFM as well as the surface roughness. Additionally, areas with different properties can be differentiated by using tapping mode AFM (James et al., 2000). WAXS is used to study the crystal structure of the polymer within nanostructured domains, while SAXS is used to study domain size of the nanophase-separated structure itself (Jokela et al., 2002). SANS is particularly powerful for characterizing hierarchical structures because contrast matching can be used to selectively examine parts of the structure using welldesigned deuteration of the polymer and/or water (Fanova et al., 2024). It has been used to identify various correlation lengths present in dry and hydrated states of AEMs and CEMs (Chan et al., 2020). An emerging technique that has similar capability to SANS, regarding selectively controlling scattering contrast, is resonant soft x-ray scattering in which the x-ray energy is tuned to specifically interact with certain elements in the IEM (Su et al., 2020; Zhong et al., 2021).

### 3.4 Ionic conductivity

In water treatment processes such as electrodialysis, an electric field is used as a driving force to induce migration of ions through IEMs. Low resistance of the IEM facilitates rapid permeation of ions. The resistance of an IEM is determined by Ohm's law and can be used to calculate ionic conductivity. The resistance of the membrane depends on the type and amount of ions present (i.e., IEC plus free ions absorbed from solution), as well as the water content and

membrane structure. Ionic conductivity can be measured using electrochemical impedance spectroscopy (EIS) where an alternating potential/voltage is applied, generally in the frequency range of 1 MHz–1 mHz, using a potentiostat. An example equivalent circuit for the ionic conductivity measurement of an IEM is shown in the inset of Figure 1C. Here,  $R_i$  and  $C_i$  represent the resistance and the capacitance at the electrode-electrolyte interfaces.  $R_b$  is the bulk resistance of the membrane, and it is determined by the x-axis intercept at high frequency. The measured  $R_b$  is used to calculate the ionic conductivity,  $\kappa$ , using Equation 4,

$$\kappa = \frac{d}{R_b A}$$
(4)

where d is the distance between electrodes, and A is the cross-sectional area through which current passes (Lazanas and Prodromidis, 2023). The determination of d and A must be consistent with the experimental set-up; two possibilities are discussed below. In practice, the area specific resistance, ASR ( $R_bA = d/\kappa$ ), dictates the performance of a membrane used in electric-field driven processes. Note that thinner membranes will yield lower ASR, which means that this metric combines the intrinsic material property of ionic conductivity with processing limitations that determine minimum achievable membrane thickness.

In membrane separation processes, the transport of ions takes place in a direction perpendicular to the surface of the membrane, and the conductivity in the thickness direction affects the actual process. Two-electrode setups, such as that shown in Figure 1A, are used for through-plane ionic conductivity measurements. The membrane is placed between two electrodes. The membrane thickness is d, and the contact area of the electrodes and the electrolyte membrane is A in Equation 4 for a two-electrode setup.

If the electrochemical properties of the IEM are isotropic, the inplane ionic conductivity can be measured using the four-electrode method. Four electrodes are arranged in parallel on the membrane surface. The two electrodes on the outsides that apply alternating current are the working electrode (WE) and counter electrode (CE),

and two electrodes in the middle are reference (Ref) electrodes where the voltage is measured. d in Equation 4 is the distance between the reference electrodes, and A is the product of wire length (w) and membrane thickness. The four-electrode method has an advantage that it is not necessary to consider the resistance of the electrode-electrolyte interfaces, because no current passes through the reference electrodes. This is particularly advantageous when the IEM is coated on a support material that would add additional resistance in the two-electrode method.

To ensure reproducibility, several things should be considered. First, the electrodes should either be blocking electrodes or allow only reversible reactions to occur. The best practice is to use platinum electrodes. Reproducible clamping pressure should be used to guarantee intimate contact between the IEM and the electrodes. To further ensure accuracy, it is a good idea to repeat measurements with various thicknesses, thus allowing the bulk membrane resistance to be separated from the interfacial resistance between the electrodes and sample that remains when extrapolating to zero thickness. This is particularly important in highly conductive IEMs. Due to the strong dependence of IEM conductivity on water content, it is extremely important to control the degree of hydration during EIS measurements. Drying of fully hydrated samples should be avoided during measurement, and other levels of hydration can be maintained by using humidity control implemented in conjunction with the EIS set-up. Stray electromagnetic fields can impact EIS measurements and can be prevented by shielding all wires. This is standard with many commercially available EIS instrumentations, often using coaxial cables for this purpose. For custom experiments, it is usually sufficient to utilize twisted pairs, whereby working and counter reference leads are twisted around each other. For highly sensitive measurements, it is necessary not only to shield the electrical leads, but also the sample cell. This is readily achieved using a Faraday cage, which is a grounded conductive housing. Finally, when reporting results it is essential that the measurement method (two-electrode or four-electrode) be specified and the dimensions reported so that both conductivity [S/cm] (an intrinsic material property) and ASR [ $\Omega$  cm<sup>2</sup>] (a membrane performance metric) can be determined.

# 3.5 Permeability and selectivity

In an IEM, selective permeation of counter-ions and exclusion of co-ions arise from the electrostatic interactions between mobile ions and fixed charged groups, a phenomenon known as Donnan exclusion. Assuming an ideal monovalent binary electrolyte, Donnan equilibrium relates concentration in the membrane to that in the external electrolyte as follows:

$$c_i^m = \frac{2(c_s^s)^2}{c_B + \sqrt{c_B^2 + 4(c_s^s)^2}}$$
 (5)

where  $c_i^m$  is concentration of free salt ions absorbed into the membrane,  $c_s^s$  is the concentration of salt in the external solution, and  $c_B$  is the bound charge concentration that is equal to swollen membrane density times IEC ( $c_B = \text{IEC} \cdot \rho_p$ ). (Hallinan and Balsara, 2013) In Figure 2A, the concentration of free co-ions in the membrane ( $c_{co-ion} = c_i^m$ ) and concentration of counter-ions in the membrane ( $c_{counter} = c_i^m + c_B$ ) are shown normalized by  $c_B$  as a function of the concentration of the

electrolyte solution ( $c_i^s$ ) with which the membrane is in equilibrium, which is also normalized by  $c_B$ . Due to the bound charges, there is a high concentration of counter-ions regardless of the external solution concentration. In contrast, co-ions only enter the membrane to a significant extent when the external solution concentration exceeds the concentration of fixed charges, i.e.,  $c_s^s/c_B \ge 1$ . In this range, the concentration of co-ions and counter-ions are similar.

Transport of water molecules and ions through IEMs is driven by osmotic pressure in forward osmosis (FO), applied hydraulic pressure in reverse osmosis (RO) or applied electric field in ED which induces an electrochemical potential gradient. In particular, transport of neutral species such as water molecules and neutral ion pairs (e.g., salt) can be driven by osmotic pressure or concentration gradient as well as hydraulic pressure for volatile species. All of these gradients induce a chemical potential gradient across the membrane. Transport of charged species (i.e., ions) can be driven by these gradients as well as electric potential gradient. All species can be rejected by structural factors such as pore size, but only ions are excluded by the fixed charge in the membrane. The overall flux of a species through the membrane,  $J_i^m$ , is described by the Nernst-Planck equation (Helfferich, 1995),

$$J_i^m = -D_i^m \left( \nabla c_i^m + z_i c_i^m \frac{F}{RT} \nabla \Phi + c_i^m \nabla \ln f_i^m \right) + c_i^m v_i^m \tag{6}$$

where  $D_i^m$  is the diffusion coefficient,  $\nabla c_i^m$  is the concentration gradient,  $z_i$  is the valence, F is Faraday's constant, R is the gas constant, T is temperature,  $\nabla \Phi$  is the electric potential gradient,  $f_i^m$  is the activity coefficient, and  $v_i$  is the velocity of species i, and superscript m indicates the membrane phase. The first term on the right-hand side is concentration-gradient-driven diffusive transport; the second term is electric-field-driven migration; the third term captures non-idealities in concentrated conditions of the membrane; and the final term is transport due to convective flow. Pressure-driven transport is not explicitly expressed in the Nernst-Planck equation, but  $f_i$  is affected by temperature and pressure.

The solution-diffusion theory describes mass transport of a species through nonporous membranes as a process involving absorption from solution to membrane, diffusion in the membrane and desorption from the membrane to external solution. This can be expressed more simply than Equation 6 for the diffusion of neutral species in a membrane, neglecting convection and assuming ideality, using Fick's first law,

$$J_i^m = -D_{ii}^m \nabla c_i^m \tag{7}$$

Helfferich derived an expression (see Equations 7, 8 in his book) that he termed "self-diffusion flux." It considers resistance to diffusion both in the membrane and in the solution boundary layer immediately adjacent to the membrane by considering equilibrium between phases. The expression comes from integrating across the regions assuming a linear concentration gradient (that is expected at steady state). A parametric representation of this self-diffusion flux in dimensionless form is shown Figure 2B, for a boundary layer velocity 200 times that in the membrane (i.e., boundary layer resistance affects only counter-ions at low concentration). This parametric representation emphasizes how IEM fixed charge content affects the flux of various components. Counter-ion flux far exceeds coion flux in ED. Water flux considerably exceeds salt flux, which is limited by co-ion transport, in RO and FO. These can be better

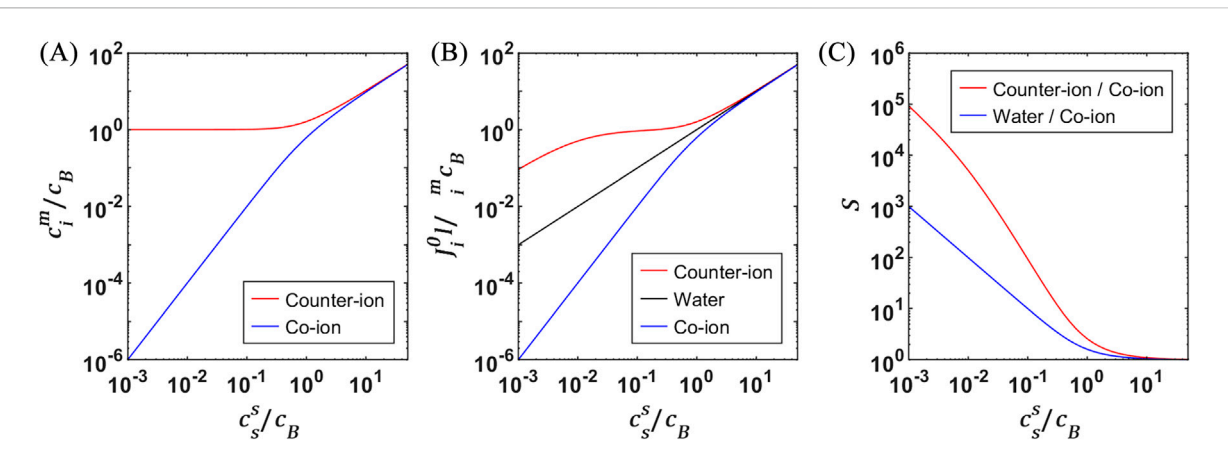


FIGURE 2
(A) Dimensionless counter- and co-ion concentrations in an IEM calculated using Donnan equilibrium for the ideal case of an IEM with monovalent counter-ions that are the same as the counter-ions in the external, binary, monovalent electrolyte. Ion concentrations in the membrane  $(c_j^m)$  are shown as a function of external salt concentration  $(c_s^s)$ , and both are normalized by the bound ion concentration in the membrane that can be calculated from the IEC and the density of the swollen membrane,  $c_B = \text{IEC}\,\rho_p$ . (B) Dimensionless self-diffusion flux,  $\frac{J_p^n}{D_p^n c_g}$ , of each ion and water as defined by Helfferich, which is a function of species self-diffusion coefficient,  $\mathcal{D}_j^m$ , and concentration gradient in the membrane, as a function of  $\frac{c_s^n}{c_s}$  (Helfferich, 1995). The concentration gradient in the membrane is estimated from  $c_j^m$  and assuming low concentration on the permeate side of the membrane. Note that  $c_s^s$  can range from very dilute up to the solubility limit, which is about 7 mol/L for NaCl in water at 25 °C. Typical  $c_B$  values for common IEMs with IECs of about 1 meq/g and densities between 1 and 2 g/cm³, range from 1 to 2 mol/L. (C) Ideal selectivities calculated from dimensionless fluxes of pure components for electrodialysis ( $S = \frac{J_{common incommon}^{n}}{J_{common incommon}^{n}}$ ) and desalination ( $S = \frac{J_{common incommon}^{n}}{J_{common incommon}^{n}}$ ) and desalination ( $S = \frac{J_{common incommon incommon$ 

visualized using selectivity (Figure 2C), which is simply the ratio of desired component (counter-ion or water) over undesired component (co-ion). From the perspective of selectivity, clearly it is desirable to maximize the IEC of IEMs, which is a challenge due to the diluting effect of increased water uptake with increasing IEC.

It is possible to explicitly express the steady-state water flux in terms of applied pressure difference ( $\Delta p$ ) by considering the pressure dependence of water chemical potential, but the flux of nonvolatile salt/ions are not effected by  $\Delta p$  (Paul, 2004; Paul, 1976). In practice, it is not the transport *within* the membrane that is of most concern, but rather what occurs in the bulk solutions on either side. Thus, it is common to take measurements of the feed/retentate, what does not pass through the membrane, and the permeate, what does pass. Flux can be written in terms of the bulk solution concentrations, if the equilibrium with the membrane is known. For condensed phases, such as aqueous electrolytes, the partition coefficient of species i is given by Equation 8.

$$K_i = \frac{c_i^m}{c_i^s} \tag{8}$$

The Equation 8 is most commonly used to quantify phase equilibrium. The permeability coefficient of species i,  $P_i$ , is the product of  $K_i$  and the *mutual* diffusion coefficient (Equation 9) that appears in Equation 7.

$$P_i = K_i D_{ii}^m \tag{9}$$

This convention means that permeability coefficient has the same units as diffusion coefficient (e.g.,  $cm^2/s$ ) and is a material property. Permeance,  $P_i/l$ , is sometimes also used to quantify transport in commercial membranes to directly account for the impact of membrane thickness on flux, analogous to the use of ASR. It is important to note that standard practice in membrane-based gas

separation is to define the permeability coefficient,  $P_{gas}$ , following Equation 10,

$$P_{gas} = \frac{J_{gas}l}{\Delta p} \tag{10}$$

which modifies the units of permeability as well as the definition of the partition coefficient (and its units) (Helfferich, 1995; Xie et al., 2010; Sagle et al., 2009) The condensed phase convention will be used throughout this review.

Permeation can be evaluated using two-chamber cells, an example of which is shown in Figure 3. For a typical experiment, one side is filled with a concentrated solution (Chamber 1, donor cell) and either pure water or a dilute solution is placed on the other side (Chamber 2, receptor cell). The two chambers are separated by the IEM whose permeabilities are in question. An approach to quantify water flux is to measure volume via the relative meniscus position in the capillary shown in inset 1 of Figure 3. This water flux can be due to an applied pressure or the osmotic pressure difference between the two solutions. In either case, water flux,  $J_w$ , is calculated by measuring the permeate volume over time relative to membrane area (Equation 11):

$$J_w = \frac{1}{A\bar{V}_{\cdots}} \frac{\mathrm{d}V}{\mathrm{d}t} \tag{11}$$

where  $\mathrm{d}V$  is the permeate volume change over time  $\mathrm{d}t$ ,  $\bar{V}_w$  is the molar volume of water, and A is the active membrane area.

Salt flux due to a concentration gradient can also be described as in Equation 12 by Fick's first law,

$$J_s^m = -D_s^m \nabla c_s^m \cong D_s^m \frac{\Delta c_s^m}{s} \cong P_s \frac{\Delta c_s^s}{s}$$
 (12)

The third and fourth expressions assume a linear concentration gradient, which is a good assumption during steady-state

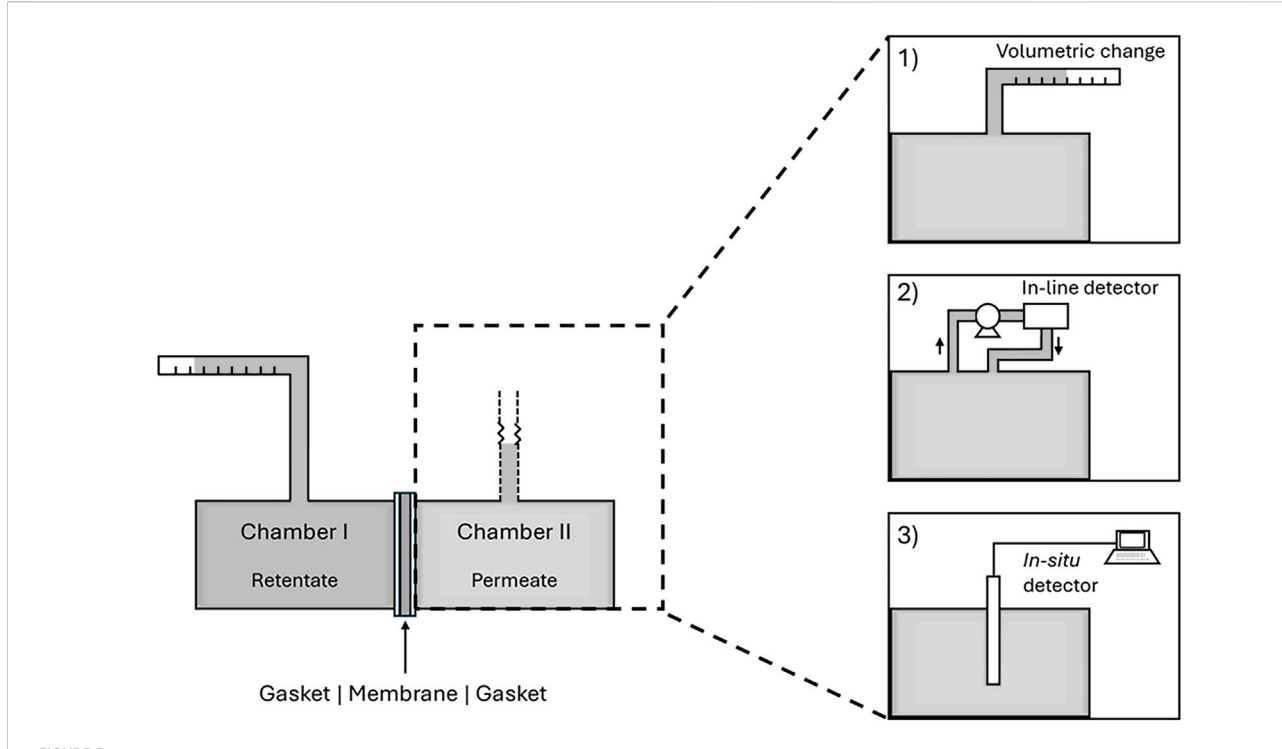


FIGURE 3
Apparatus for permeation measurement. A concentration, electric field, or pressure gradient is applied across the membrane. The feed/retentate side (Chamber I in this schematic) is at higher electrochemical potential for the transporting species, and the permeate side (Chamber II) is at lower electrochemical potential, which drives permeation across the membrane (from Chamber I to Chamber II). For the case of a concentration gradient, Chamber I is filled with a concentrated solution and Chamber II is filled with a dilute solution. Various detection strategies can be employed to measure change in variables such as volume, concentration, or conductivity using 1) graduated capillaries for volume change, 2) a detector in-line with a circulating closed loop to/from Chamber II, or 3) an in-situ detector. Examples of in-line and in-situ detectors include spectroscopy, conductivity and pressure measurement.

permeation. The final equality assumes that the partition coefficient is constant, i.e., not a function of concentration. Ion permeability can also be determined using a two-chamber permeation setup. As salt diffuses through the membrane from donor to receptor cell, the diffused salt gradually increases the conductivity of the receptor cell. Conductivity is recorded over time, e.g., via inset 2) or 3) in Figure 3, and used to calculate the salt concentration using a calibration curve. The salt permeability  $P_s$ , can be calculated as in Equation 13:

$$-\frac{V_r l}{2A} \ln \left[ 1 - \frac{2c_r(t)}{c_d(0)} \right] = P_s t \tag{13}$$

where  $c_r(t)$  is the salt concentration in the receptor cell at time  $t, c_d(0)$  is the initial concentration of salt in the donor cell, and  $V_r$  is the volume of the receptor cell (Oh et al., 2018). It is best practice to equilibrate the membrane with the same solution concentration used to charge the donor cell, for example, 1 mol/L aqueous salt solution. This can be combined with water uptake measurements discussed above. The receptor cell is most commonly pure water, but it may be necessary to include a low concentration of salt, e.g., to prevent irreversible swelling or dissolution of developmental membranes.

In order to handle multicomponent transport in nonideal charged electrolytes, including membranes, it is necessary to use a system of equations similar to the Stefan-Maxwell framework that was first developed by Onsager, but rather than considering gradients of chemical potential, it is necessary to consider electrochemical potential. Mass balance, current flow, and electroneutrality

equations are needed to solve the coupled set of flux equations. The reader is referred to Newman's book for a detailed description of this system and to Geise, Paul, and Freeman's article for application specifically to membranes (Newman and Thomas-Alyea, 2004; Geise et al., 2014b).

Selectivity is generally defined as the ratio of flux of a desired species to that of an undesired species. The selectivity of an IEM is often quantified by its ability to preferentially exclude co-ions while facilitating the transport of counter-ions, but it could also apply to the ability to differentiate two different types of counter-ions or even the transport of neutral species such as water and methanol. Precisely engineered IEMs discussed below demonstrate selectivity not only between counter-ions and co-ions but also among counter-ions with differing valences. This selectivity is critical for the efficiency and performance of various electrochemical and separation processes, including redox flow batteries, desalination, and electrodialysis. Selectivity for different polar, neutral molecules or for different ions of the same valence remains a challenge in IEM design.

Permselectivity,  $\alpha$ , is most commonly calculated using pure component permeability coefficients,  $\alpha_{i/j} = P_i/P_j$ . Although, actual selectivity may be considerably different when the membrane is challenged with a multicomponent mixture. This definition is general and can be applied to any type of membrane-based separation, for neutral or charged species. Ion selectivity, specifically for ED, can also be calculated from transference

numbers, although the definition of selectivity varies in reported expressions (Helfferich, 1995). Selectivity as defined in this review for transport driven purely by electric field is simply the ratio of desired to undesired ion (Equation 14).

$$\alpha_{i/j} = \frac{t_i^m}{t_i^m} \tag{14}$$

where  $t_i^m$  and  $t_j^m$  are the transference numbers of species i and j in the membrane, respectively. The ion transference number is defined as the fraction of current carried by that species. Various methods to calculate and measure the ion transference number have been reported (Geise et al., 2014a; Hittorf, 1899; Price, 1998; Kwon and Lee, 2020; Vasylkevych and Slisenko, 2019). A rapid method to determine the membrane transference number involves measuring the membrane potential. In this approach, the IEM is placed in an electrochemical cell in which each side is filled with the same type of electrolyte solution, but at different concentrations. The resulting membrane potential ( $\Delta E$ ) is measured, and the  $t_+^m$  is calculated (Nagarale et al., 2006) (Equation 15):

$$\Delta E = \left(2t_{+}^{m} - 1\right) \frac{RT}{zF} \ln \frac{a_c}{a_d} \tag{15}$$

where  $a_c$  and  $a_d$  are the activities of the concentrated and dilute solutions, respectively. An ideal CEM has  $t_+=1$  where only cations transport through the membrane and all anions are excluded. A transference number of 0.5 indicates equal mobility of cations and anions. Practically complete exclusion of co-ions cannot be achieved, but it is desirable to design membranes with  $t_+$  as close to unity as possible.

# 3.6 Thermal and mechanical properties

The thermal properties of IEMs are important not only for high-temperature applications such as fuel cells, but also for setting temperature conditions during membrane fabrication and assessing thermal degradation (Bébin and Galiano, 2006a; Bébin and Galiano, 2006b; Yao and Wilkie, 1999). Thermogravimetric analysis (TGA) is used to measure water content, assess chemical decomposition, and evaluate thermal stability. In polymer-based IEMs, weight loss is observed as temperature increases due to the evaporation of water, decomposition of ion-exchange functional groups, degradation of the polymer backbone, and combustion of the polymer.

Glass transition temperature  $(T_{\rm g})$  and melting temperature  $(T_{\rm m})$  are two other important thermal properties. Below  $T_{\rm g}$ , the membrane is glassy and permeating species move through the free volume. Glassy materials tend to have a high modulus and fail in a brittle fashion. Above  $T_{\rm g}$ , the membrane is rubbery and transport is coupled with segmental dynamics if the membrane is not highly swollen (Geise et al., 2014b). Segmental dynamics correlate with how far the operating temperature is above  $T_{\rm g}$ . Rubbery materials tend to have a low modulus and exhibit toughness due to failing at large strains. In either case (glassy or rubbery), reinforcement is often required and can be achieved by various means that include porous support, combination of glassy and rubbery microdomains, crosslinking, or crystallinity. Semicrystalline polymers tend to have desirable mechanical properties due to the inclusion of rigid crystallites in a flexible amorphous matrix. Crystallinity is lost at  $T_{\rm m}$ . This may or may

not be desirable, for although crystals yield a mechanical benefit, they also block the transport of permeants. Differential scanning calorimetry (DSC) is used to analyze the crystallinity,  $T_{\rm m}$  and  $T_{\rm g}$  of polymers. Exoand endothermic heat flow are measured as a function of temperature while heating or cooling the specimen at a constant rate. The heat flow is recorded relative to an inert reference under identical conditions.

The mechanical performance of IEMs can be significantly affected by the nature and concentration of solvents and salts, as they are typically operated in electrolyte-saturated environments. Ion-exchange and separation processes require the membrane to maintain sufficient mechanical robustness to withstand physical and chemical stress during operation. Since most IEMs swell upon water absorption, resulting in reduced mechanical strength, they are commonly supported with a reinforcing substrate or backing layer to enhance durability and dimensional stability. To fabricate free-standing membranes, crosslinked polymers, block copolymers, or polymer blends (Hosseini et al., 2012) are employed as mentioned earlier. The mechanical properties of polymers are characterized by tensile and puncture strength using a universal testing machine (UTM) or by rheological analysis using dynamic mechanical analysis (DMA).

Table 1 represents the thermal, physical and mechanical properties of charged polymers for IEMs. The properties of neutral polymers were included for comparison. Quaternization of amorphous polymer backbones decreases  $T_{\rm g}$  (or  $T_{\rm m}$ ) due to bulky and flexible side chains while sulfonation increases  $T_g$  due to the rigid aromatic rings in the functional groups and strong molecular interaction. Quaternized PEEK shows increased  $T_{\rm g}$  compared to neutral material, but it is lower than  $T_{\rm m}$  of PEEK and this behavior is due to the chain flexibility and crystallinity of PEEK. The thermal, physical and mechanical properties of IEMs vary greatly depending on the type of functional groups and counterions. For example, sulfonated PSf with sodium form exhibited notably higher  $T_g$ (310 °C) compared to its acid form (225 °C). Due to the hydrophilicity of IEMs, hydration also largely impacts on the thermal properties and, consequently, the processability. The influences of thermal properties and hydration on the membrane preparation are further discussed in Section 4.

Charged polymers showed lower tensile modulus and tensile strength than neutral polymers. The change of thermal and mechanical properties must be considered when designing manufacturing procedure. For example, for melt processing, film fabrication with neutral polymer followed by functionalization seems to be preferable because of lower  $T_{\rm g}$  and higher mechanical strength to avoid thermal decomposition of the functional groups or film failure during the manufacturing.

# 4 Processing techniques

Conventional and emerging membrane processing techniques are introduced. The comparison of IEMs prepared with different processing methos is given in Table 2.

# 4.1 Solution casting

Solution casting is a method to form membranes by evaporating solvent from a polymer solution that is spread on a substrate. This

TABLE 1 Thermal, physical and mechanical properties of IEM materials.

Polymer	IEM type	$T_{\rm g}$ ( $T_{\rm m}$ )	IEC	WC	E	σ	$\epsilon_{b}$	Reference
		°C	meq/g	%	GPa	MPa	%	
PS	-	100	-	-	3.4	50	2.5	a
	CEM	115-140	5.3-7.0	45-70	-	41-45	-	b,c
PSf	-	180-190	-	-	2.6	70	50-100	a,d
	CEM	225-310	1.3-2.2	20-80	1.2	38.6	-	d-f
	AEM	187.9	1.0-1.7	-	-	30-50	3–19	g
PAES	-	221	-	-	1.3	65	32	h
	CEM	205-273	1.4-2.1	19.4	1.7	44-57	11-15	i,j
	AEM	112-170	1-1.9	9.6	-	-	-	k,l
PPO	-	220	-	-	2.4	66	20-60	a
	CEM	235	2.5	24-177	0.8-1.2	30-60	-	m
	AEM	-	1.0-2.5	11-112	0.2-0.8	7-31	8-32	n-p
PEEK	-	143 (334)	-	-	3.9	175	70	a
	CEM	201.5	2.5	98	0.8	45	160	P
	AEM	240	1.4-1.6	33	0.9	67	14	r

PS: polystyrene; PSf: polysulfone; PAES: poly (arylene ether sulfone); PPO: poly (2,6-dimethyl-1,4-phenylene oxide); PEEK: poly (ether ether ketone);  $T_g$ : glass transition temperature;  $T_m$ : melting temperature; IEC: ion exchange capacity; WC: water content; E: tensile modulus;  $\sigma$ : tensile strength;  $\varepsilon_b$ : elongation at break. Functionality of CEMs includes sulfonated or disulfonated acids or sodium forms. Functionality of AEMs includes quaternary ammonium or imidazole compounds with hydroxide or chlorine forms.

\*(Fried, 2014),  $^b$ (Bellinger et al., 1994),  $^c$ (Stránská et al., 2018),  $^d$ (Noshay and Robeson, 1976),  $^c$ (Bébin and Galiano, 2006a),  $^t$ (Swaby et al., 2023),  $^b$ (Yang et al., 2012),  $^b$ (Oroujzadeh et al., 2015),

"(Fried, 2014), "(Bellinger et al., 1994), "(Strånskå et al., 2018), "(Noshay and Robeson, 1976), "(Bebin and Galiano, 2006a), "(Swaby et al., 2023), "(Yang et al., 2012), "(Oroujzadeh et al., 2015), "(Oh et al., 2014), "(Venkatachalam et al., 2023), "(Xim et al., 2020), "(Behbahani et al., 2023), "(Yang et al., 2019), "(Wu et al., 2015), "(Yang et al., 2016), "(Parnian et al., 2017), "(Shang et al., 2021).

method can be used for either charged or neutral polymers. In the latter case, neutral polymer is ionized by chemical modification in the solid state after forming a membrane (Xie et al., 2012). The surface and morphological properties of solution-cast membranes depend on the properties of the solvent/polymer such as miscibility (Bridge et al., 2022a), solvent volatility (Bridge et al., 2022a; Fischer et al., 2023), and solution viscosity (which is affected by choice of solvent, molecular weight of polymer, and solution composition) (Bridge et al., 2022a; Kruczek and Matsuura, 2003). Important casting conditions include the use of a doctor blade or other spreading method, cast solution thickness (which affects the resulting membrane thickness), and substrate temperature (Yee et al., 2013). Polymer chains can be aligned by flow, e.g., when using a doctor blade, which results in anisotropic transport properties and can reduce the amount of water swelling (Simari et al., 2021). It is particularly important to consider the surface energy between the solution and the substrate. It must be sufficiently favorable for the solution to wet, but also sufficiently low to release the dry membrane. Various approaches can be used to facilitate release of the membrane from the substrate, such as dewetting the membrane with a nonsolvent or, in laboratory scale research, dissolving away the substrate with a preferential solvent. Finally, solvent removal is an important consideration that can be achieved by drying (e.g., with heat and vacuum), by exposing the solution to a non-solvent (often referred to as phase inversion), or by "activation" with another reagent that extracts residual solvent, e.g., via osmotic pressure. The third approach was used to remove residual solvent by soaking sPEEK membranes in 1 mol/L sulfuric acid, and found to be crucial for achieving optimal membrane properties (Jun et al., 2012).

In solution casting and other membrane formation methods, surface interactions can also affect membrane surface roughness and porosity. These include interaction between the solution and the substrate, as well as interactions between polymer and inorganic particles that are sometimes used in membranes. For example, shrinkage was found to be more significant when solutions of PSf in N-methylpyrrolidone were spread on hydrophobic substrates such as Teflon than when spread on hydrophilic substrates such as glass. The increased shrinkage resulted in lower water permeability. In this study, the membranes were formed from solution by immersion precipitation, rather than solvent evaporation (Aerts et al., 2006). Anisotropic micromorphology can appear when casting heterogeneous IEMs using nanofillers or via NIPS, based on the gravimetric effect and solution viscosity. Hierarchical membranes can be produced using the formation of anisotropic distribution of components (Bakangura et al., 2016; Liu et al., 2017; Bridge et al., 2022a).

Yee et al. studied the effect of casting parameters on the degree of sulfonation (DS), IEC, swelling, film thickness and electrochemical properties. The DS, IEC and swelling showed temperature-dependence. The thickness of dry films ( $d_{\rm film}$ ) cast by doctor blade exhibited linear relationship with the product of cast thickness ( $d_{\rm cast}$ ) and polymer weight fraction in casting solution ( $\omega_{\rm polymer}$ ), as shown in Figure 4 (Yee et al., 2013). The DS, IEC, swelling, and electrochemical property were independent of membrane thickness. The optimal thickness of the IEMs can be selected based solely on mechanical stability, ease of handling, and the specific design requirements of the application. It should be

TABLE 2 Comparison of IEMs prepared with different processing methods.

Method	Solution casting	Paste method	Extrusion	Electrospinning	Phase inversion
Membrane structure	Supported/free-standing Dense/porous	Heterogeneous Dense Cross-linked Dispersed in matrix	Homogeneous/heterogeneous Dense/porous Single/multilayered	Homogeneous Porous	Homogeneous Porous
Thickness range (µm)	20-170 <sup>a-f</sup>	128-200 <sup>k-m</sup>	135-200 <sup>q-s</sup>	78-130 <sup>x</sup>	10-200 <sup>af-ah</sup>
Roughness (nm)	$R_a = 0.69-34.8^g \\ R_q = 0.98-423^{g,h}$	$R_a = 10.8^{n}$ $R_q = 19-27^{o}$ $R_z = 89-123^{o}$	sd = 2-10 <sup>q</sup>	0.5-16 <sup>y-aa</sup>	$S_a = 4.16 - 5.26^{ah}$ $S_z = 32.4 - 73.6^{af}$
Attainable IEC windows (meq/g)	0.3-2.5 <sup>b-f</sup>	1.17-3.5 <sup>k-m</sup>	0.59-1.62 <sup>s,t</sup>	0.42-5.8 <sup>x,y,ab,ac</sup>	0.65-2.5 <sup>af,ah,ai</sup>
Hydrated conductivity (mS/cm)	3-130 <sup>a,b,d</sup>	3.5-10.3 <sup>m</sup>	0.7-43 <sup>r-t</sup>	0.24-4.5 <sup>x,ac</sup>	0.072-9.07 <sup>af,ah,ai</sup>
Swelling (%)	20-36 <sup>a,c,i,j</sup>	6-26 <sup>p</sup>	60-77 <sup>s-v</sup>	40-100 <sup>x,y,ab,ac</sup>	4-9 <sup>aj</sup>
Young's modulus (GPa)	15.4-34.3 <sup>d</sup>	0.2 <sup>n</sup>	0.15–0.5 (MD) <sup>s</sup> 0.02–0.2 (TD) <sup>s</sup>	0.3-1.1 <sup>ac</sup>	0.02-0.78 <sup>ag</sup>
Residual solvent/VOC (%)	3.0-4.8 <sup>g</sup>	n.f.	<2.0 <sup>A</sup> ,w	<1.0 <sup>ad,ae</sup>	n.f.
Surface cost	\$ 432–495/m <sup>2</sup> B	\$ 135/m <sup>2</sup> C	\$690-1,363/m <sup>2</sup> D	n.f.	n.f.

Ra: arithmetic average roughness; Ra: root-mean-square roughness; Rz: maximum peak to valley height; sd: standard deviation of surface profile; Sa; arithmetic mean height of the surface; Sz: maximum height of the surface; MD: machine direction; TD: transverse direction; n.f.: not found.

"(Luo et al., 2021), b(Xie et al., 2012), c(Yee et al., 2013), d(Simari et al., 2021), c(Slade et al., 2010), b(Deboli et al., 2022), b(Kruczek and Matsuura, 2003), b(Domhoff and Davis, 2020), d(Fischer et al., 2023), d(Mokrini et al., 2010), b(Alexandrova and Iordanov, 1995), d(Alexandrova and Iordanov, 2001), d(Nokrini and Mizutani, 1981), d(Alexandrova and Iordanov, 2011), d(Cakmak and Simhambhatla, 1995), d(Bébin and Galiano, 2006b), d(Mokrini and Huneault, 2006), d(Polat and Sen, 2017), d(Choi et al., 2007), d(Mokrini et al., 2010), d(King et al., 2013), d(King et al., 2013), d(Kirioglu et al., 2014), d(Kirioglu et al., 2024), d(Nam et al., 2017), d(Kirioglu et al., 2024), d(Kirioglu et al., 2011), d(King et al., 2014), d(King et al.

noted that for maximum flux through the membrane, extremely thin membranes are desired that lack sufficient mechanical strength to be free standing. Therefore, thin selective layers on porous supports and fiber-reinforced composites are prevalent in industrial use.

Xie et al. examined how pretreatment and counter-ion type affect water and ion transport in solution-cast disulfonated poly(arylene ether sulfone) (BPS) films (Xie et al., 2012). The membrane was treated with acid, heat, and ion-exchange in different manners. Soaking in sulfuric acid increased water uptake and permeability, while thermal treatment in water enabled tuning of transport properties. Boiling in sulfuric acid had the most pronounced effect, greatly enhancing water and salt transport. Counter-ion effects were minor compared to thermal treatment. Overall, the permeability and selectivity followed the expected trade-off relationship.

Slade et al. investigated the influence of processing methods on WC and resistivity by recasting extruded Nafion with different solvents, butan-1-ol and propan-2-ol (Slade et al., 2010). The recast Nafion membrane showed higher water uptake and lower resistivity than extruded membranes implying reorientation of ionic domains (Gebel, 2000). The different behavior of water content and resistivity was explained by the different physical properties of solvents: boiling point, vapor pressure and viscosity that changes evaporation rate affecting organization of microstructure.

Technical challenges of solution casting lie in the long evaporation time, difficulty of thickness control, and anisotropic microstructure. Accurate control of thickness is challenging due to the solution fluidity even when the solution is cast using a doctor blade (Yee et al., 2013; Harris and Walczyk, 2006; Chede et al., 2018). This problem can be addressed by using viscous solvent or higher polymer concentration, but extensive evaporation time, high temperature or vacuum are required to completely remove residual solvent. Faster evaporation using volatile solvent or heating can be considered, but it can cause defects, rough surface, and even breakage of the membrane (Bridge et al., 2022a).

Other strategies to evenly spread viscous solutions on support films are nip roller extrusion and slot die extrusion (Harris and Walczyk, 2006). These techniques can be applied to continuous process of solution casting (Chede et al., 2018; Siemann, 2005). The viscoelastic properties of the solution and the surface adhesion of the roller material were found to be key parameters to produce defect-free membranes with uniform thickness (Siemann, 2005; Harris and Walczyk, 2006). In slot die extrusion, critical processing parameters include flow rate, substrate speed, slot gap, etc., all of which must be precisely controlled to ensure uniform film quality.

# 4.2 Paste method

The paste method is the most widely used manufacturing process for the mass production of hydrocarbon-based IEMs (Mizutani, 1990). A paste solution is filled into a bath and coated onto a backing membrane to form a composite membrane that is wound onto a winding roll, as shown schematically in Figure 5. The paste solution contains monomers with functional groups, crosslinkers, initiators, and additives such as powders for

<sup>&</sup>lt;sup>A</sup>Residual diluent in membrane extruded with diluent, after extraction.

<sup>&</sup>lt;sup>B</sup>Nafion N211, N212.

<sup>&</sup>lt;sup>C</sup>Neosepta CMX.

<sup>&</sup>lt;sup>D</sup>Nafion N115, N117, N424, N438.

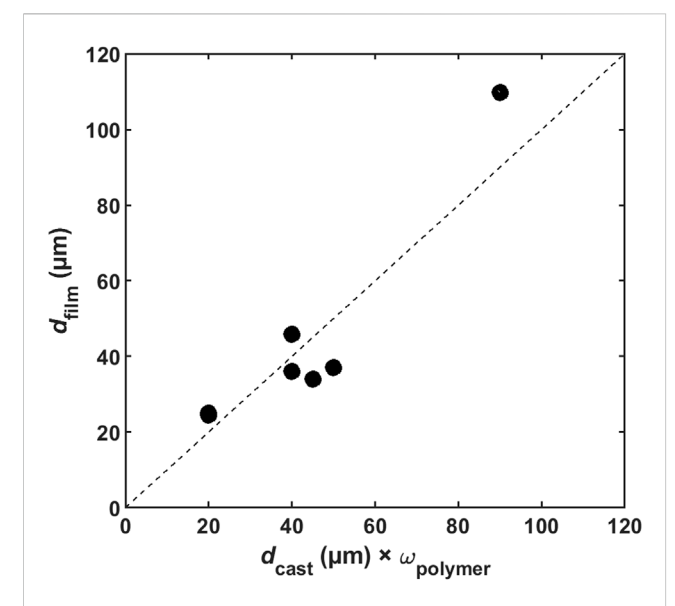
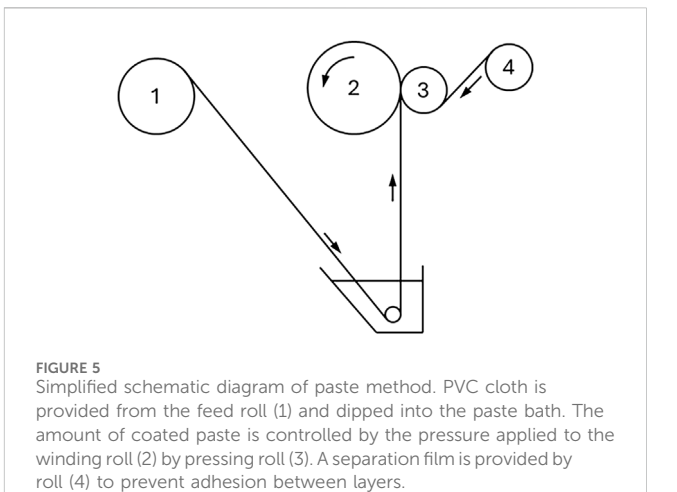


**FIGURE 4** Relationship between dry membrane thickness ( $d_{film}$ ) and the product of solution cast thickness ( $d_{cast}$ ) times polymer concentration in solution ( $\omega_{polymer}$ , in weight fraction). Dashed line represents  $d_{film} = d_{cast}\omega_{polymer}$ . If polymer and solution densities are known, volume fraction can be used to improve accuracy of the prediction (Data from reference Yee et al. (2013)).

mechanical strength or rubber for flexible properties. Polyvinylchloride (PVC) fibers or porous membranes (e.g., porous polyethylene films) are used as backing membranes. After winding, the roll is detached and undergoes thermal treatment to polymerize and crosslink the monomers in the paste. Two different types of composite membranes are used. For many applications, such as reverse osmosis, flux is of paramount importance such that the functional layer formed by the paste must be very thin (e.g., 100 nm). Transport through this thin dense layer occurs by the solution diffusion method, which provides the selectivity needed (e.g., to reject salt). In other applications in which selectivity is more important, such as electrodialysis, the IEM formed by the paste percolates through the entire porous support, providing longer transport pathways to take advantage of differences in the mobility of the species to be separated (e.g., counter-ions and coions). In either type of composite membrane, the primary role of the porous support is to provide mechanical integrity.

The percolated structure of the composite membrane is determined by the composition, miscibility and solubility of the components (Mizutani, 1990). Like the solution casting method, neutral monomers can be used that are subsequently converted into an IEM after forming the composite membrane, or charged monomers can be used to directly fabricate a composite IEM. Mizutani et al. demonstrated that IEMs prepared by the paste method exhibited a finely interpenetrating network of PVC and ion-exchange resin, where the microphase-separated structure (≤50 nm) and controlled swelling through PVC confinement significantly enhances conductivity, mechanical stability, and overall membrane performance (Mizutani and Nishimura, 1970; Mizutani and Ikeda, 1987).

Another study of interpenetrating structure of PVC/styrene-divinylbenzene (St-DVB) was conducted in which St-DVB was incorporated into porous PVC supports and then treated to add



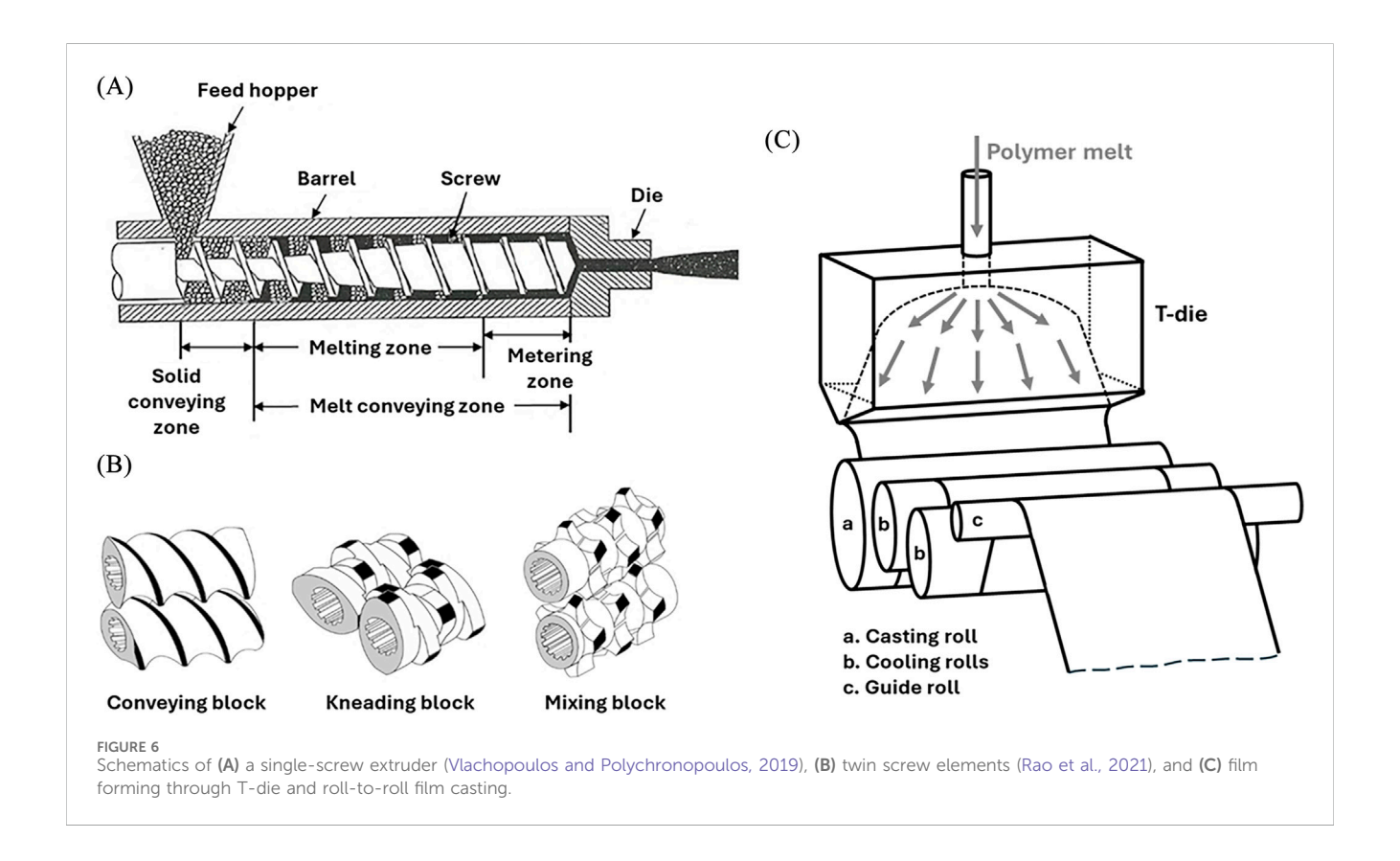
ionic functionality via sulfonation (to form a CEM) or quaternization (to form an AEM) (Mizutani, 1990). The authors used TEM to visualize the distribution of crosslinked St-DVB in the interconnected micropores of the PVC gel. With increasing PVC pore volume fraction (Neosepta CL-25T < Neosepta CH-45T < Neosepta C66-5T), greater charge density could be formed in the composite membrane due to higher content of St-DVB. This resulted in larger IEC, higher water content, and lower resistance (Hori et al., 1986). The crystallinity of PVC in the backing materials and base membranes was not affected by the presence of ion-exchange resin (Mizutani and Ikeda, 1987). The authors claimed that the crystallites of PVC acts as crosslinking points to some extent providing dimensional stability and toughness to the membrane while still achieving high IEC.

The relationship between transport properties and crosslinking density in composite IEMs has been investigated by Sudoh and coworkers (Sudoh et al., 1990a; Sudoh et al., 1990b). The effect of crosslinking density was examined by correlating it with the volume fractions of pores, polyelectrolyte, and inert polymer. A model indicated that it is desirable to maximize the volume fraction of polyelectrolyte while selecting a backing material with reduced inert polymer volume fraction. It was found that there is an optimum point of crosslinking that maximizes polyelectrolyte volume fraction. In combination with the optimal backing material, the membrane conductivity approached that of the external solution (Sudoh et al., 1990a; Sudoh et al., 1990b; Alexandrova and Iordanov, 2001).

The paste method is technologically mature and used in large-scale manufacturing processes. However, it has several limitations due to the necessity of using a backing membrane: 1) the volume fraction of the polyelectrolyte phase is less than 50%, 2) the ionic conductivity is below  $10^{-2}$  S/cm, and 3) the overall membrane thickness is greater than 150 µm (Tanaka et al., 2011). Additionally, it requires extensive post-processing time–polymerization for greater than 10 h and ionization for more than 10 h (Sudoh et al., 1990a; Tanaka et al., 2011).

# 4.3 Extrusion

Commercial PE or polypropylene (PP) battery separators and PFSA IEMs are produced via extrusion (Kusoglu and Weber, 2017;

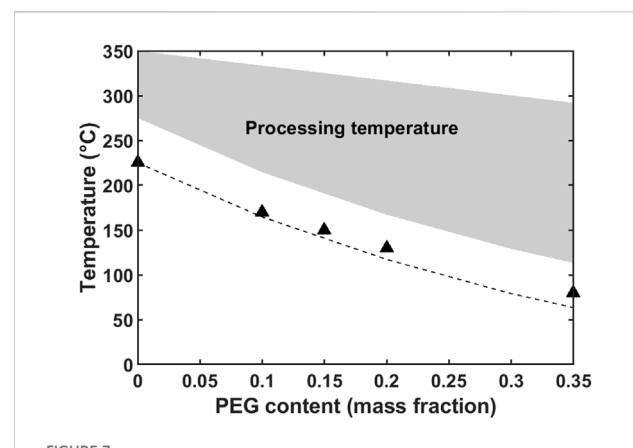


Jana et al., 2018). Extrusion is a conventional polymer processing technique used to blend (Kim K. et al., 2023), compound (Eker et al., 2002) and shape (Rosato, 1998) thermoplastic polymer products. It is a continuous in-line process to profile polymeric materials including melting, mixing, conveying and profiling of the polymer and roll-to-roll processing of films (Hays and Pokorski, 2025).

Common extruders can be categorized by screw types: single-screw extruder (SSE) and twin-screw extruder (TSE). SSEs are preferable for the manufacturing of profiles or sheets that require stable output, whereas TSEs offer superior mixing capabilities. Figure 6 shows schematic images of an SSE, screw elements of TSEs, and the process of film formation through a T-shaped die (T-die) followed by roll-to-roll film casting. Polymers in pellet, powder or granule form are provided by a feeder and proceed from the conveying zone to melt and mixing zone (Figure 6A). In polymer blends and composites, additional components such as secondary polymer or inorganic fillers can be pre-mixed or introduced via a side feeder. The polymer melt needs to be compressed to maintain consistent thickness profile. The compression is achieved through screw design (SSE) - typically by increasing the screw diameter in the metering zone (Figure 6A) - or screw configuration (TSE) which involves various assembly of screw elements (Figure 6B). The polymer melt is extruded through T-die to form films (Figure 6C). The T-die has to be carefully designed considering the thermodynamic and rheological properties of the materials and processing parameters such as throughput and pressure drop. The film orientation is determined by the flow rate and casting roll speed. The cooling rate, determined by the cooling roll temperature and roll speed, significantly affects the film's degree of crystallinity, which in turn influences its mechanical strength. The films are wound on a roll after trimming the edges with non-uniform thickness.

Extrusion has merits of being a scalable and solvent-free process, but it is an energy-intensive technique due to the high thermal and mechanical energy required. Homogeneous membranes can be reinforced by extruding with additives or fillers. Heterogeneous membranes can be manufactured by blending polymers. The distribution and morphology of heterogeneous membranes are determined by material properties such as polymer blend miscibility and melt viscosity, and processing parameters such as processing time, barrel temperature and screw configuration. The temperature range must be carefully selected due to the thermal sensitivity of the IEM components such as plasticizer and sulfonate groups, particularly when scaled up, where increased retention time of the materials and viscous heating from higher machine torque exacerbate thermal stress (Bébin and Galiano, 2006a; Oh et al., 2014).

Bebin and Galiano demonstrated film extrusion of glassy sulfonated PSf (sPSf) using a low-molecular-weight poly(ethylene glycol) (PEG) as plasticizer to improve the processibility (Bébin and Galiano, 2006a; Bébin and Galiano, 2006b). The use of 20% plasticizer effectively depressed the glass transition temperature ( $T_g$ ) of the acid form sPSf/PEG blends, from 225 °C to about 100 °C, and reduced the minimum melt processing temperature (Bébin and Galiano, 2006a). In Figure 7, filled areas indicate the safe processing temperature range for a sodium form sPSf/PEG blend. The upper limit of the processing temperature was determined by TGA where weight loss was less than 10%. In addition to improving processability, increased amount of plasticizer increased the porosity



Determination of processing temperature of a sPSf/PEG blend. Data from Bébin and Galiano (2006a).  $T_{\rm g}$  of the blends from experiment (triangles) and estimation using Fox equation (dashed line) are shown. The grey region represents extrusion temperature ( $T_{\rm g}$  + 50 °C). The upper limit was estimated by the decomposition temperature (350 °C and 300 °C at 0 and 0.3 PEG weight fraction, respectively) (Bébin and Galiano, 2006b).

of the membrane after solvent extraction (Bébin and Galiano, 2006a; Bébin and Galiano, 2006b; Oh et al., 2017b) resulting in increased water uptake and ionic conductivity, but decreased selectivity (Bébin and Galiano, 2006a; Oh et al., 2018). Interestingly, the durability of the membrane in hot water was significantly affected by the processing method, where extruded membranes lasted two to three times longer than solvent cast membranes.

A comparative study of solution-cast Nafion (NR211) and extruded Nafion (N117) was conducted by Peron and coworkers (Peron et al., 2010). Isotropic swelling and conductivity were observed in NR211. Whereas, extrusion causes stress-induced orientation of Nafion chains in N117 that results in anisotropic swelling. Swelling is greater in the transverse directions, where the backbone distance between neighboring polymer chains is limited by weak van der Waals forces, than in the extrusion direction, where backbone bonds limit swelling. The water permeability of NR211 was higher than N117, despite the hydration number being lower, and the oxygen diffusion coefficient was also affected by membrane processing method. The hydration numbers of as-received NR211 and N117 at 25 °C were 12 and 22 mol<sub>H2O</sub>/mol<sub>SO3</sub>, respectively. The significant differences in membrane properties caused by membrane preparation method highlights the importance of processing in membrane-based applications.

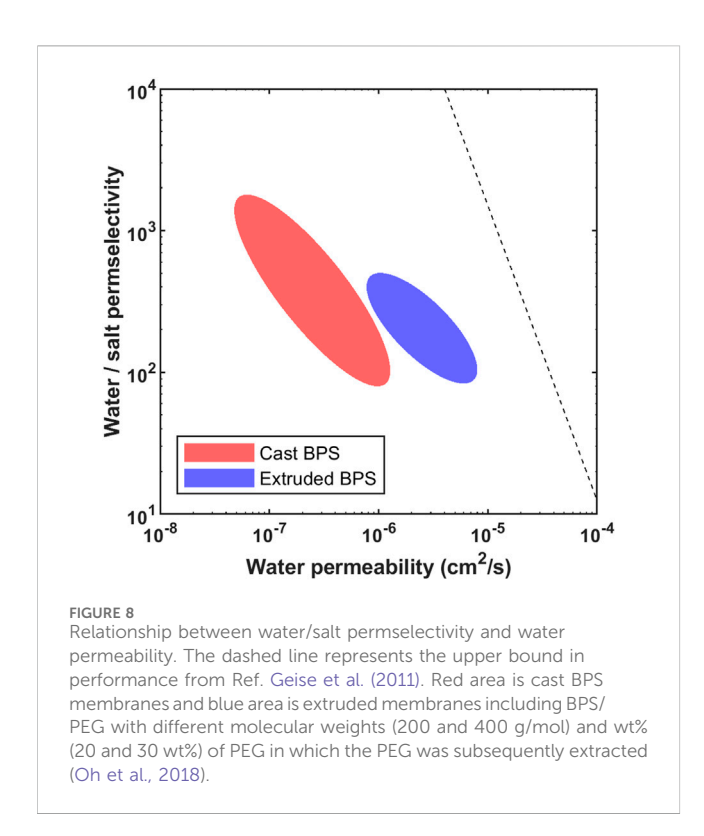
A systematic study of the dependence of IEM permselectivity on the processing history was conducted by Oh and coworkers (Oh, 2015). Single-layer IEMs of BPS were prepared by extrusion using PEG as plasticizer which was extracted using water after forming films (Oh et al., 2017a). At least 20 wt% PEG was used to obtain defect-free, uniform membranes. The water-soluble PEG was completely extracted from the extruded film, indicating the potential for preparing CEMs using extrusion (Oh et al., 2017a), while BPS/PEG blends prepared by solution casting did not exhibit PEG extraction (Lee et al., 2011). Although the solution-casting study used slightly higher molecular weight PEG (600 compared to 400 g/mol), it is not clear why different processing methods led to this dramatic difference. Lee and coworkers did note that PEG was

retained after 150 days in 30 °C deionized water due to the strong dipole-ion interaction between the potassium counter-ions of the sulfonate groups and ethylene groups in PEG. The extruded BPS polymer membrane demonstrated the expected trade-off between water permeability and water/salt selectivity (Figure 8). Notably, the extruded membrane showed higher water permeability but reduced selectivity compared to neat BPS membranes produced by solution casting. These findings indicate that processing history alone can significantly alter both permeability and selectivity.

One drawback of extrusion is the high processing temperature required for melt processing, which can increase the risk of thermal degradation of charged polymers (Bébin and Galiano, 2006a; Oh et al., 2014). Charged polymers in their acid form typically exhibit poorer thermal stability compared to their neutral or metal salt counterparts. A strategy to address this problem that was discussed above is to ionize neutral polymer films in the solid state, e.g., after extrusion. In another study by Mokrini et al., sulfonic acid moieties were incorporated into a polymer blend membrane of PVDF and styrene-(ethylene-butylene)-styrene (SEBS) triblock copolymer (Mokrini and Huneault, 2006; Mokrini et al., 2006). Interface modification was carried out by adding 1 - 5 wt% of acrylate block copolymers to improve the miscibility of two polymers. Scanning electron microscopy (SEM) analysis revealed that the incorporation of the acrylate block copolymers markedly reduced phase segregation and enhanced mechanical properties with as little as 1 wt% of compatibilizer. The IEC and ionic conductivity increased with increasing SEBS and compatibilizer contents while exhibiting similar or lower water uptake.

Due to the hydrophilicity of charged polymers, moisture not only impacts the transport performance of IEMs as discussed previously, but it also plays a significant role in processing. Bulejko et al. reported aggravated screw torque and extruder head pressure with increased moisture (10-25% moisture) in sulfonated polystyrenedivinylbenzene (sPS-DVB)/low density polyethylene (LDPE) blends (Bulejko and Stránská, 2018). sPS-DVB with various moisture contents (from 2% to 25%) was blended with LDPE using an extruder to prepare pellets. These pellets were then formed into membranes via another extrusion. The specific mechanical energy (SME) and pressure of a twin-screw extruder reached a stable steady state during processing with low-moisture resins. However, moisture contained in the pellets caused instabilities in SME and head pressure as well as uneven resin content in the pellets, possibly due to inhomogeneous mixing and formation of resin agglomerates in the gravimetrically controlled feeder caused by increased electrostatic interactions. These effects translated to slightly decreased IEC in the membranes and higher membrane resistance that was able to be partially overcome by pressing. This demonstrates that various processing parameters are important in extrusion of IEMs, including relative humidity, which is not typically considered when extruding hydrophobic thermoplastics.

Compared to other manufacturing methods, extrusion offers a significant advantage in terms of mixing performance. Hybrid membranes using inorganic nanofillers can be used to improve mechanical strength, durability, thermal stability and conductivity. Mokrini et al. studied the effect of processing methods of SiO<sub>2</sub>/Nafion hybrid CEMs produced by extrusion and solution casting (Mokrini et al., 2010). Significantly improved dispersive mixing was observed from extrusion mixing due to the high shear stress that

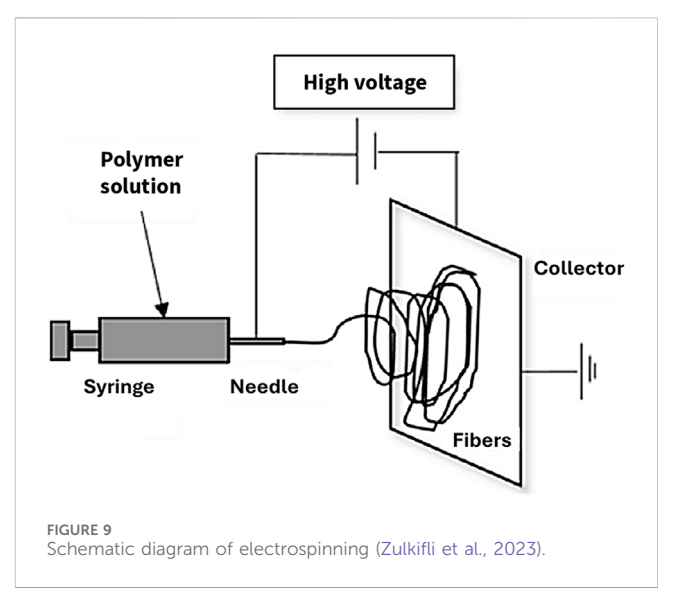


helps to effectively reduce particle size and break aggregates. At high temperature (80 °C) and low relative humidity (<50%), conditions used for fuel cell operation, melt-extruded samples were found to exhibit higher conductivity than membranes prepared by casting.

# 4.4 Electrospinning

Electrospinning is a processing technique to make fiber mats by applying high voltage between an electrically conductive nozzle/ needle and a conductive substrate/collector located at some distance from the nozzle. A schematic diagram is presented in Figure 9. Polymer solution is ejected from the nozzle forming a Taylor cone. A stream of solution is accelerated from the tip of the Taylor cone due to effect of the electric field on charged and dipolar components of the solution. The acceleration causes the stream to thin and the solvent evaporates rapidly due to the high speed and narrow diameter of the stream, forming a polymer fiber that then impinges on the surface of collector, forming a fiber mat that can be used as a porous membrane. The structural characteristics of the mat such as pore size, porosity, tortuosity, and active surface area are determined by material and processing parameters such as the composition of the polymer solution, feed rate, applied voltage, and the distance between the nozzle and the collector. The structure of the fiber mat impacts the membrane properties such as water uptake, IEC, permeability, selectivity and ionic conductivity. The electrospun membrane can be directly fabricated from ion-exchange resins via electrospinning, or alternatively, a porous electrospun membrane can be used as a supporting membrane and subsequently pore-filled with ion-exchange resin (Kim S. et al., 2023).

Chakrabarty et al. fabricated a nanofiber IEM of sPEEK by electrospinning onto a non-woven PP fabric (Chakrabarty et al.,

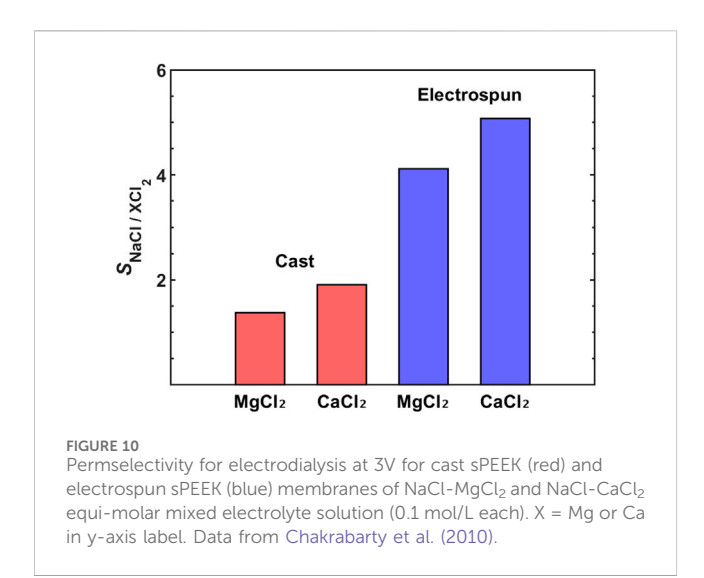


2010). The selectivity of the membrane to Na $^+$  over Mg $^{2+}$  or Ca $^{2+}$  was evaluated. As shown in Figure 10, compared to cast sPEEK membranes, the electrospun sPEEK membrane exhibited remarkably higher selectivity (2.5–3 times that of cast sPEEK) for Na $^+$  over Mg $^{2+}$  and Ca $^{2+}$ , due to restriction of divalent cations by the nanofibrous pores or nanochannels in electrospun sPEEK.

Reves-Aguilera et al. studied the influence of electrospinning parameters on the permeation properties of blends of polyepichlorohydrin (PECH) and polyacrylonitrile (PAN) AEMs (Reyes-Aguilera et al., 2021). PECH was simultaneously crosslinked and functionalized with cations via reaction with solution-cast triethylenediamine. Despite higher IEC than membranes, electrospun membranes showed hydrophobicity (lower swelling degree), possibly due to the increased surface energy caused by air bubbles trapped within the fibrous mesh, which is reflected in the larger contact angle of the electrospun membranes. Electrospinning parameters of humidity, flow velocity, and collector rotational speed were also investigated. The most significant effect was due to collector rotational speed, with higher RPM resulting in some fiber alignment and reduced degree of swelling. However, the impact on permselectivity was not significant. Interestingly, the electrospun membranes exhibited a decrease in thickness after thermal treatment while the fiber diameter remained unchanged. Surface roughness increased after thermal treatment, suggesting that the fibers in the thermally treated membrane were more densely packed. This was supported by the thermally treated membranes exhibiting a lower degree of swelling and slightly improved permselectivity to anions over cations.

# 4.5 Phase inversion

Phase inversion, also known as NIPS, is widely used to form asymmetric membranes. A polymer solution (dope) is exposed to a nonsolvent for the polymer that is miscible with the solvent in the solution. At the surface, the polymer rapidly precipitates forming a thin, dense selective layer (Bridge et al., 2022a). As shown in Figure 11, porosity forms in the bulk of the dope due to the



presence of the good solvent and the slow diffusion of nonsolvent causing gradual precipitation of the polymer. This kinetic process results in a gradient of porosity and pore size, with small micropores immediately adjacent to the dense layer, providing robust support and transitioning to a hierarchy of pores, including macropores, at the opposite surface of the asymmetric membrane that facilitates rapid bulk transport to or from the dense selective layer.

Garmsiri et al. fabricated asymmetric AEMs using NIPS with chloromethylated PES for cadmium removal from wastewater. The IEC was controlled by varying the chloromethylation time (6, 9, and 24 h) (Garmsiri and Mortaheb, 2015). The NIPS process used DMAc as the solvent and deionized water as the non-solvent. Quaternization was performed by immersing the membrane in a trimethylamine solution, followed by ion-exchange of Cl- with OH- in a base solution. The fabricated AEM exhibited a structure consisting of large channels penetrating the membrane and smaller pores in the channel walls. The pore size increased with rising IEC, accompanied by an increase in porosity. This behavior is attributed to the influence of the membrane's charge density on the interaction between the solvent and non-solvent during membrane formation. Due to the larger pore size and higher porosity, water uptake increased with increasing IEC. Electrochemical properties such as membrane potential, transference number, and ionic conductivity also improved with increasing IEC. A hybrid liquid membrane was used to extract CdI<sub>4</sub><sup>2-</sup> ions from wastewater. The hybrid liquid membrane consisted of an organic liquid phase contained between two AEMs. Unlike in typical IEM applications, the permselectivity was found to increase with increasing IEC in the hybrid liquid membrane system. This was due to the hopping mechanism of CdI<sub>4</sub><sup>2-</sup> ions along the organic-liquid-filled pores of the AEMs, which does not accompany water transport. Compared to nonionic PVDF membranes, the porous PES-based AEM demonstrated superior cadmium removal.

Wet-phase inversion was used to prepare a porous IEM by Kim et al. (2014). PVDF was dissolved in DMF and non-solvent was added to the solution. A membrane was obtained by evaporating the solvent and non-solvent after casting. The porous PVDF membrane was grafted with styrene and sulfonated using sulfuric acid. The porous PVDF-based IEM showed higher IEC and ionic conductivity and comparable  $t_{+}$  compared to Nafion.

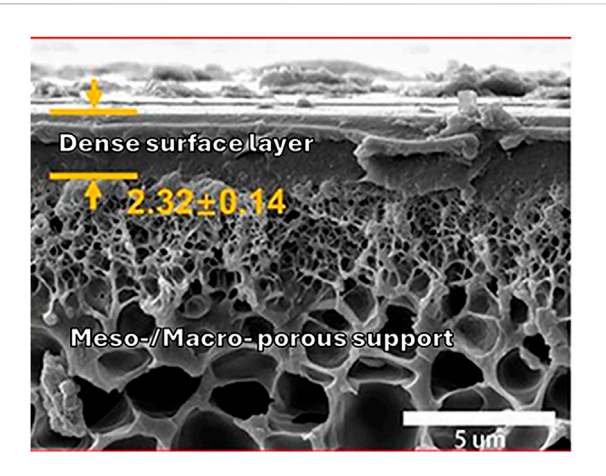


FIGURE 11
Cross-sectional SEM of an asymmetric membrane formed by
NIPS of a solution of PSf in a good solvent mixture of
dimethylacetamide (DMAc) and tetrahydrofuran exposed to ethanol as
a nonsolvent. Adapted from Mei et al. (2020).

# 4.6 Emerging methods

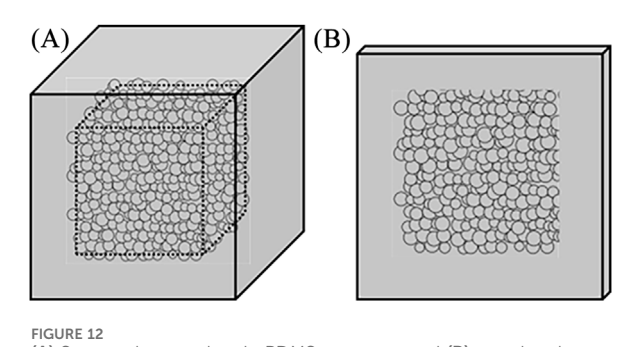
Festarini et al. reported a novel method to fabricate a porous polydimethylsiloxane (PDMS) support membrane using a sugar template (Figure 12) (Festarini et al., 2017). Sugar powder with uniform size obtained by sieving was dried and molded into sugar cubes. A liquid PDMS precursor was infiltrated into the sugar template and subsequently crosslinked. The sugar was then extracted with deionized water forming micropores in the PDMS matrix. The IEM was fabricated by pore-filling Nafion into the PDMS pores. This technique offers several advantages: it avoids the use of toxic organic solvents, allows easy control of pore size by adjusting the particle size of sugar, and forms a uniform pore structure. However, a notable drawback is that the PDMS must be sliced using a microtome to produce the membrane. Due to the viscoelasticity and flexibility of PDMS, membranes thinner than 200 µm cannot be fabricated using this method.

# 5 Charged membranes in energy and sustainability

In this section, the current research status of charged polymer membranes in industrial applications for mineral mining (e.g., lithium extraction) from concentrated brines and electronics waste (e.g., batteries and semiconductors) is presented. The requirements of applications and processing levers are summarized in Table 3.

# 5.1 Lithium extraction from battery waste

Lithium separation and extraction are typically achieved through solubility-based processes such as precipitation or chemical leaching. These processes require large infrastructure and generate chemical waste resulting in significant



(A) Sugar cube template in PDMS precursor and (B) cured and sliced porous membrane after extracting sugar. Described approach used in Festarini et al. (2017).

environmental impacts. ED is a membrane-based separation technology that separates ionic components under electrochemical current. ED is used for treatment of wastewater, brackish water, and industrial effluent, and can also be applied to produce lithium salts from brines, ores, and waste lithium-ion batteries, particularly from cathode leachate (Al-Amshawee et al., 2020; Gurreri et al., 2020). Most lithium extraction studies using ED focus on primary resources such as sea water (Ying et al., 2023; Yang et al., 2025), and studies targeting battery recycling wastewater are limited (Foo and Lienhard, 2025). This subsection introduces membrane-based lithium extraction technologies from battery wastewater.

With the exception of protons, lithium ions tend to have slightly higher permeability than other cations in low water content CEMs, but in highly swollen CEMs sodium ion permeability can exceed that of lithium ions due to sodium's smaller hydration shell and thus higher hydrated ion mobility. (Castro et al., 2025) in either case, the permselectivity of lithium over sodium is close to one, which presents a challenge for selective separation. The more promising approach to selectively concentrate lithium ions appears to be recovery in the permeate. To achieve this, Wamble et al. developed a model to optimize multistage diafiltration (membrane-based filtration using continuous dilution) for the effective separation of Li<sup>+</sup> and Co<sup>2+</sup> ions in Li-ion battery recycling based on membrane properties (Wamble et al., 2022). This process uses lithium-selective nanofiltration membranes ( $S_{Li/Co} = 32$ ) at each stage allowing

lithium to pass more easily than cobalt. As a result, the permeate is enriched in lithium, while the retentate becomes cobalt-rich. Retentate is recycled between stages, diluted to prevent membrane fouling and can be recovered as a cobaltrich product from the final stage. The permeate stream moves forward to the next stage as part of the feed, and lithium-rich product is collected at the last stage. An ideal membrane for this process would have high Co2+ rejection, high Li+ permeability, chemical stability, and resistance to fouling, in order to minimize membrane area required to achieve effluent targets. In an alternative approach, Baird et al. developed a membrane composed of a sulfonated PIM (sPIM), which is selective for Na+ and K+ over Li+ (Baird et al., 2025). They investigated ion permselectivity driven by electrochemical overpotential across brines under various device architectures. When the selectivity was normalized by concentrations of each ion (Na+ or Li+) in the brine, Na+/Li+ selectivity reached 3.03, enabling the removal of 29% of Na<sup>+</sup> and 41% of K<sup>+</sup> from a brine solution within 1 h, while extracting only 9.5% of Li<sup>+</sup>, resulting in a lithium-enriched effluent.

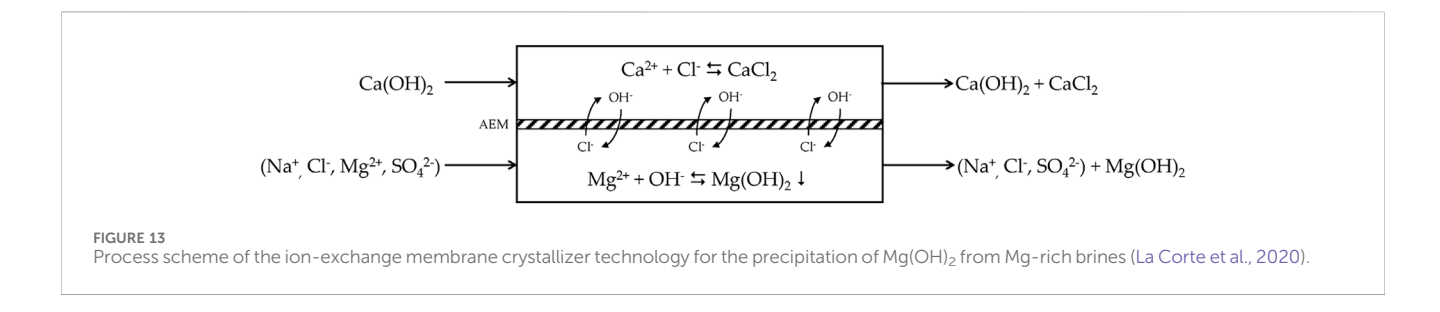
A lithium recovery method has also been developed in which Li $^{\scriptscriptstyle +}$  is converted into LiOH after first concentrating it as Li $_2\text{CO}_3$  (Hyder et al., 2025). Hyder et al. studied the direct recovery of lithium from battery recycling wastewater using both standard ED and bipolar membrane electrodialysis (BPED). These two processes were combined to concentrate lithium ions and convert them into LiOH. Commercial Fujifilm Type 12 AEM, Fujifilm Type 12 CEM and PCCell BPM were used. Lithium in the form of Li $_2\text{CO}_3$  present in the wastewater was concentrated using standard ED, then converted into LiOH using BPED. The lithium concentration in the recovered solution increased by 58% compared to the original wastewater using ED, and an additional 67% increase was achieved through BPED, yielding LiOH with purity over 96%.

# 5.2 Mineral mining from brine concentrates

Concentrated brines discharged from desalination plants contain significantly higher salinity than seawater, offering greater economic potential from mineral recovery (1.5–2.5 times compared to seawater) (Sharkh et al., 2022). Despite its significant potential and growing attention, research on mineral mining from concentrated brines is still at an early stage (just over a decade)

TABLE 3 Requirements of applications and processing levers.

Application	Requirements	Processing levers
Lithium extraction from battery waste	High Li <sup>+</sup> selectivity Chemical resistance to acids and solvents Low swelling Mechanical robustness	Interpenetrated structure Multilayered membrane Cross-linking Surface coating/modification
Mineral mining from brine concentrates	High ion selectivity Durability in high salinity Anti-fouling	Cross-linking Surface coating/modification
Mineral recovery from semiconductor waste	High permeability High ion selectivity Chemical resistance to reagents Anti-fouling	Porous membrane Multilayered membrane Cross-linking Surface coating/modification



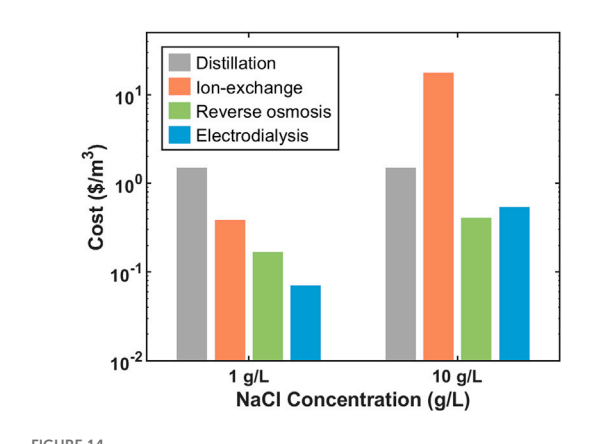


FIGURE 14
Water desalination costs per volume of potable water at two different feed salt concentrations for distillation, ion-exchange, RO and ED. Cost for distillation is not influenced by salt concentration. For ion-exchange, RO and ED, cost increases with increasing salt concentration, following a power law dependence. The most cost-effective desalination method is ED at low salt concentration and RO at high salt concentration. Data from Ho and Sirkar (2012).

(Gurreri et al., 2020), and pilot-scale brine treatment using ED mostly has focused on desalination, with mineral mining considered a potential byproduct (Oren et al., 2010; Xu et al., 2018). Minerals present in concentrated brine include bromine, magnesium, potassium, calcium, sodium, lithium, strontium, rubidium, and boric acid. Separation technologies using ED have been investigated to selectively remove monovalent ions such as Na $^+$  and Cl $^-$  from multivalent ions such as Ca $^{2+}$ , Mg $^{2+}$  and SO $_4$  $^{2-}$ .

The separation performance is determined by the selectivity and permeation. At low salt concentration, the selectivity is dominated by the acidity of the functional groups, electronegativity of counterions and hydration level of the membranes, rather than IEC (Münchinger and Kreuer, 2019). The different nature of counterions can also lead to different behavior of Donnan exclusion at higher molarity due to different binding strength. For example, small, hard cations with high charge density such as Li+ have a strong hydration shell that does not participate in membrane hydration. This increases the concentration of fixed charge (c<sub>B</sub>) and thereby lowers lithium ion uptake due to enhanced Donnan exclusion (Equation 5). However, Cs+ ions (large, soft ions with delocalized charge) bind strongly with the fixed charge groups and eventually "neutralize" the membrane and weaken Donnan effect at high salt concentration. Therefore, the coion concentration in the aqueous phase of membrane is close to the salt concentration in the external solution. The effect of ionic strength has been studied by Galizia et al. in cross-linked sPS-DVB copolymer membrane using cations with different sizes and valences (Li<sup>+</sup>, Na<sup>+</sup>, K<sup>+</sup>, Mg<sup>2+</sup> and Ca<sup>2+</sup>) (Galizia et al., 2017). This study on ion sorption showed higher ion sorption, lower water uptake and weaker Donnan potential with increasing ion size, counter-ion valence, and concentration of external solution.

Selective ion separation in brine with high salinity is also influenced by fouling occurring both on the membrane surface and within its internal structure (Dammak et al., 2021). The presence of organic, inorganic, and ionic components can accumulate on the surface and/or in pores resulting in lower flux and higher resistance, making processes such as ED less efficient and therefore less competitive. Electrostatic interactions are the primary mechanism that attracts foulants to IEMs. In particular, the presence of strongly hydrated cations such as Ca<sup>2+</sup> and Mg<sup>2+</sup> can progressively replace weakly hydrated ions like Na<sup>+</sup> and Cl<sup>-</sup> within the pores of IEMs, leading to an increase in the proportion of bound water. As a result, the amount of free water within the membrane decreases, osmotic pressure rises, and the polymer matrix swells, which reduces mechanical strength and increases the effective pore radius-ultimately compromising ion selectivity. Over prolonged operation, heterogeneous membranes are especially prone to reduced adhesion between ion-exchange resins and inert binders due to swelling, resulting in the formation of macropores and increased free water content, which further accelerates fouling. Therefore, selective ion separation under high-salinity conditions would benefit from membranes with tight channel morphology and a matrix that robustly resists swelling.

Careful consideration of these factors in membrane material selection and structural design is crucial for fouling mitigation and long-term operational stability. As mentioned in the Extrusion section, electrospun sPEEK membranes exhibited nanofibrous pore structures that hinder the transport of divalent cations, thereby enabling selective separation between monovalent and divalent cations (Chakrabarty et al., 2010). The separation of cadmium ions using AEMs has also been previously discussed in the Electrospinning section (Garmsiri and Mortaheb, 2015). In such cases, selective permeation through the AEM is facilitated by the transport of negatively charged complexes via a supported liquid membrane (SLM) process. Ion selectivity in SLM has been observed to increase with IEC, which also enhances ion permeability. In addition, ion-exchange membrane crystallization (IEMC) has emerged as a potential technique for mineral recovery (La Corte et al., 2020). As illustrated in Figure 13, the concentration gradient and Donnan potential across the AEM drive counter-transport of Cl<sup>-</sup> and OH- ions, leading to the recovery of CaCl2 in one stream and crystallization-induced precipitation of Mg(OH)<sub>2</sub> in the other stream.

# 5.3 Mineral recovery from semiconductor waste

The semiconductor manufacturing process consists of several steps, including wafer fabrication, oxidation, photolithography, etching, deposition and ion implantation, metallization, electrical die sorting, and packaging. As various chemical substances are used in each stage, semiconductor wastewater has a complex chemical composition, making it particularly difficult to treat. Compared to other types of industrial wastewater, research on semiconductor wastewater treatment remains relatively underdeveloped. In particular, studies on treating semiconductor wastewater using IEMs are extremely limited (Sim et al., 2023).

Wang et al. employed ED with commercial CEM and AEM to treat developer wastewater generated from photolithography process which contains high alkali matter (Wang et al., 2013). The main ingredient in the developer is tetramethylammonium hydroxide (TMAH), but the developer waste also contains some extent of mineral content including alkali metals. After ED with current density of 30 mA/cm², the TMAH was concentrated for recovery and demineralized, removing for example, 94% of potassium and nearly 50% of iron and sulfur.

Su et al. employed ED combined with ultrafiltration (UF) to treat copper chemical mechanical planarization (Cu-CMP) wastewater generated during semiconductor processing (Su et al., 2014). To mimic the composition of actual Cu-CMP wastewater, commercial silica slurries were diluted, and the turbidity and UF flux of the permeate water were measured. While the permeate flux increased with decreasing particle concentration, the particle removal rate remained above 99.7%, regardless of the concentration. The subsequent ED process achieved 99.3% Cu<sup>2+</sup> removal when operated at 1.5 V/cm for 3 h. The Cu<sup>2+</sup> ions adsorbed into the CEMs were effectively recovered using 3 wt% hydrochloric acid.

# 6 Conclusion

Membrane-based separation is a promising technology for mineral recovery from industrial waste, offering a more sustainable alternative to conventional methods like precipitation and distillation due to its lower energy consumption and operating costs (Figure 14). Charged membranes are essential in separation processes because their selective ion transport enables efficient recovery of specific valuable metals from complex industrial waste streams. While much research has focused on synthesis methods, the processing of charged membranes remains underexplored and is often addressed only as a subtopic in existing literature. Yet, processing is crucial for tuning membrane structure and enhancing properties such as permeability, conductivity, and ion selectivity. In this review, the manufacturing technology of charged polymer membranes were explored, including solution casting, paste method, extrusion, electrospinning, and phase inversion. Each method presents distinct advantages and limitations in terms of controlling charge density, thickness uniformity, and mechanical strength, which are critical to membrane performance and durability under harsh conditions. To select the appropriate membrane preparation method, one must consider the properties of the polymer being used to form the membrane, the operating conditions and the application-specific separation requirements. For example, to concentrate brine, a method that yields a charged, porous membrane will provide high water flux needed with reasonable ion rejection. On the other hand, final recovery of a specific element will likely be better achieved with ED, and a method that provides a dense membrane with high IEC (and thus good selectivity) is desired. Proper selection of polymer, membrane processing method, and separation technique will enable more efficient, scalable, and environmentally responsible resource utilization.

There are numerous other considerations involved in scaling up membrane technologies that were not addressed in this review, but that those working in industry must consider. These include pressurization and pumping, membrane module design, pre- and post-treatment of solutions, and membrane maintenance. Pressurization is important for any sieving-based separation, such as nanofiltration through porous IEMs as a pretreatment to concentrate desalination brine or aqueous battery waste streams, but it is also used in reverse osmosis where the pressure difference causes a concentration gradient in the membrane that is essential for solution-diffusion based separation. Pumping is another important consideration, because boundary layer resistance (i.e., concentration polarization) is directly correlated with flow rate across the surface of the membrane, with higher flow rates decreasing the thickness of the boundary layer (Hallinan, 2009). High flow rates can also be favorable to minimize membrane fouling due to bacteria and other solids deposition. On the other hand, high flow rates increase operational costs associated with power consumption. Membrane modules come in four main types: tubular, plate and frame, hollow fiber and spiral wound. Refer to Baker's book for schematics and discussion of the advantages and disadvantages of each type (Baker, 2012). Various considerations are inherent in preand post-treatment that relate to prevention of fouling and membrane degradation, such as chlorination and de-chlorination (Geise et al., 2010). Membrane maintenance and periodic replacement is necessary to remove foulants, that significantly decrease permeate flux over time, and to address pin holes that eventually develop in active separation layers of solution-diffusion type membranes.

The outlook for membranes is promising due to their ability to efficiently and continuously separate challenging waste, such as concentrated desalination brine and battery waste. Their existing ability to separate monovalent ions from multivalent ions (even in porous IEMs) is a major strength, as this opens the possibility for separately recovering lithium salts/carbonates from rare earth and other multi-valent metal ions that are present in lithium-ion battery There are exciting opportunities for process intensification by combining membrane separation with other processes, either in series or in hybrid formats (Chen et al., 2020). Hybrid formats include, for example, membrane-liquid extraction, membrane distillation, and membrane bioreactors. Reducing membrane costs, increasing operational efficiency and lifetime, and discovering new applications to improve process sustainability using membranes will require collaborative innovation to develop new polymer chemistries, to design optimal membrane processing techniques, and to model module formats and efficient process control. As emerging membrane applications of resource recovery from battery waste and brine are developed and application-specific criteria become clear, it will be important to complete the loop by quantitatively mapping the processing-structure-property relationships

discussed in this review with performance metrics required by these emerging applications. Achieving this connection will require that the recommended standardized protocols be used for measuring membrane properties. The standardized characterization of membranes will offer a solid basis for the complex challenge of developing IEMs for practical applications where multiple separation techniques may be combined, and membrane performance-property relationships depend on the coupled aspects of materials and processing.

# **Author contributions**

KK: Data curation, Methodology, Conceptualization, Writing – original draft, Writing – review and editing, Visualization. DH: Visualization, Funding acquisition, Validation, Supervision, Writing – review and editing, Conceptualization.

# **Funding**

The author(s) declare that financial support was received for the research and/or publication of this article. This work was made possible by funding from the inaugural Florida State University President's Sustainability and Climate Solutions grant program.

# References

Adams, B. A., and Holmes, E. L. (1935). Adsorptive properties of synthetic resins. J. Soc. Chem. Ind. 54, 1-6. doi:10.1002/jctb.5000540214

Aerts, P., Genné, I., Leysen, R., Jacobs, P. A., and Vankelecom, I. F. J. (2006). The role of the nature of the casting substrate on the properties of membranes prepared via immersion precipitation. *J. Membr. Sci.* 283, 320–327. doi:10.1016/j.memsci.2006.

Aghaei, A., Islam, M. A., Jashni, E., Khalili, A., Cho, J.-Y., and Sadrzadeh, M. (2024). Efficient lithium recovery from water using polyamide thin-film nanocomposite (TFN) membrane modified with positively charged silica nanoparticles. *ACS Appl. Mater. Interfaces* 16, 66514–66531. doi:10.1021/acsami.4c15939

Aguilar-Sanchez, A., Jalvo, B., Mautner, A., Rissanen, V., Kontturi, K. S., Abdelhamid, H. N., et al. (2021). Charged ultrafiltration membranes based on TEMPO-oxidized cellulose nanofibrils/poly(vinyl alcohol) antifouling coating. *Rsc Adv.* 11, 6859–6868. doi:10.1039/d0ra10220b

Al-Amshawee, S., Yunus, M. Y. B. M., Azoddein, A. A. M., Hassell, D. G., Dakhil, I. H., and Hasan, H. A. (2020). Electrodialysis desalination for water and wastewater: a review. *Chem. Eng. J.* 380, 122231. doi:10.1016/j.cej.2019.122231

Alexandrova, I., and Iordanov, G. (1995). Copper (II) transfer through carboxylic ion-exchange membranes prepared by paste method. *J. Appl. Polym. Sci.* 57, 1315–1318. doi:10.1002/app.1995.070571108

Alexandrova, I., and Iordanov, G. (2001). Transport of cobalt and zinc through a carboxylic membrane based on poly (vinyl chloride)/poly (methyl metacrylate-codivinylbenzene) system. *J. Appl. Polym. Sci.* 80, 47–50. doi:10.1002/1097-4628(20010404)80:1<47::AID-APP1073>3.0.CO;2-W

Arges, C. G., Parrondo, J., Johnson, G., Nadhan, A., and Ramani, V. (2012). Assessing the influence of different cation chemistries on ionic conductivity and alkaline stability of anion exchange membranes. *J. Mater. Chem.* 22, 3733–3744. doi:10.1039/C2JM14898F

Baird, M. A., Kingsbury, R. S., Wang, Y., Zhu, C., Chen, G., Klivansky, L., et al. (2025). Electrochemical Li+ enrichment of mixed-cation brines with antiselective polymer membranes. *ACS Energy Lett.* 10, 3500–3507. doi:10.1021/acsenergylett. 5c01120

Bakangura, E., Cheng, C., Wu, L., He, Y., Ge, X., Ran, J., et al. (2016). Highly charged hierarchically structured porous anion exchange membranes with excellent performance. *J. Membr. Sci.* 515, 154–162. doi:10.1016/j.memsci.2016.05.059

Baker, R. W. (2012). "Membranes and modules," in Membrane technology and applications. 3rd ed. (UK: Wiley).

# Conflict of interest

The authors declare that the research was conducted in the absence of any commercial or financial relationships that could be construed as a potential conflict of interest.

# Generative AI statement

The author(s) declare that no Generative AI was used in the creation of this manuscript.

Any alternative text (alt text) provided alongside figures in this article has been generated by Frontiers with the support of artificial intelligence and reasonable efforts have been made to ensure accuracy, including review by the authors wherever possible. If you identify any issues, please contact us.

# Publisher's note

All claims expressed in this article are solely those of the authors and do not necessarily represent those of their affiliated organizations, or those of the publisher, the editors and the reviewers. Any product that may be evaluated in this article, or claim that may be made by its manufacturer, is not guaranteed or endorsed by the publisher.

Bandehali, S., Moghadassi, A., Hosseini, S. M., Parvizian, F., Ghanbari, D., Rahimizadeh, R., et al. (2024). Smart ion exchange membrane with high impact in heavy metals separation prepared by electrospinning process with ultrasensitive responsiveness for water treatment. *Chem. Eng. Res. Des.* 205, 763–774. doi:10.1016/j.cherd.2024.04.028

Banerjee, S., and Curtin, D. E. (2004). Nafion® perfluorinated membranes in fuel cells. J. Fluor. Chem. 125, 1211–1216. doi:10.1016/j.jfluchem.2004.05.018

Bauer, B., Strathmann, H., and Effenberger, F. (1990). Anion-exchange membranes with improved alkaline stability. *Desalination* 79, 125–144. doi:10.1016/0011-9164(90) 85002-R

Bébin, P., and Galiano, H. (2006a). Processing of PEMFC membranes by extrusion: part 1. Sulfonated polysulfone in acid form. *Adv. Polym. Technol. J. Polym. Process. Inst.* 25, 121–126. doi:10.1002/adv.20066

Bébin, P., and Galiano, H. (2006b). Processing of sulfonated polysulfone for PEMFC membrane applications: part 2. Polymer in salt form. *Adv. Polym. Technol. J. Polym. Process. Inst.* 25, 127–133. doi:10.1002/adv.20067

Behbahani, H. S., Mithaiwala, H., Marques, H. L., Wang, W. S., Freeman, B. D., and Green, M. D. (2023). Quaternary ammonium-functionalized Poly(Arylene ether sulfone) random copolymers for direct air capture. *Macromolecules* 56, 6470–6481. doi:10.1021/acs.macromol.3c00760

Beigmoradi, R., Samimi, A., and Mohebbi-Kalhori, D. (2021). Controllability of the hydrophilic or hydrophobic behavior of the modified polysulfone electrospun nanofiber mats. *Polym. Test.* 93, 106970. doi:10.1016/j.polymertesting.2020.106970

Bellinger, M. A., Sauer, J. A., and Hara, M. (1994). Deformation and tensile fracture behaviour of sulfonated polystyrene ionomers: effects of counterion and excess neutralizing agent. *Polymer* 35, 5478–5482. doi:10.1016/s0032-3861(05)80011-4

Bridge, A. T., Pedretti, B. J., Brennecke, J. F., and Freeman, B. D. (2022a). Preparation of defect-free asymmetric gas separation membranes with dihydrolevoglucosenone (CyreneTM) as a greener polar aprotic solvent. *J. Membr. Sci.* 644, 120173. doi:10.1016/j.memsci.2021.120173

Bridge, A. T., Santoso, M. S., Maisano, J. A., Hillsley, A. V., Brennecke, J. F., and Freeman, B. D. (2022b). Rapid macrovoid characterization in membranes prepared via nonsolvent-induced phase separation: a comparison between 2D and 3D techniques. *J. Membr. Sci.* 661, 120923. doi:10.1016/j.memsci.2022.120923

Brijmohan, S. B., Swier, S., Weiss, R., and Shaw, M. T. (2005). Synthesis and characterization of cross-linked sulfonated polystyrene nanoparticles. *Industrial Eng. Chem. Res.* 44, 8039–8045. doi:10.1021/ie050703v

Bryjak, M., Pozniak, G., and Kabay, N. (2007). Donnan dialysis of borate anions through anion exchange membranes: a new method for regeneration of boron selective resins. *React. Funct. Polym.* 67, 1635–1642. doi:10.1016/j.reactfunctpolym.2007.07.028

- Bulejko, P., and Stránská, E. (2018). The effect of initial moisture content of cation-exchange resin on the preparation and properties of heterogeneous cation-exchange membranes. *Mater. Chem. Phys.* 205, 470–479. doi:10.1016/j. matchemphys.2017.11.049
- Cakmak, M., and Simhambhatla, M. (1995). Dynamics of uni and biaxial deformation and its effects on the thickness uniformity and surface roughness of poly (ether ether ketone) films. *Polym. Eng. Sci.* 35, 1562–1568. doi:10.1002/pen. 760351910
- Castro, S., Ssekimpi, D., Tang, Y., and Hallinan, D. (2025). Transport in perfluorosulfonic acid (PFSA) membranes: effects of pretreatment, side-chain length, and alkali metal cation. *Front. Membr. Sci. Technol. Sec. Membr. Modul. Process.* 4, 1681118. doi:10.3389/frmst.2025.1681118
- Cath, T. Y., Chellam, S., Katz, L. E., Kim, J., Breckenridge, R., Macknick, J., et al. (2021). *National alliance for water innovation (NAWI) industrial sector technology roadmap* 2021. Golden, CO, United States: National Renewable Energy Lab.
- Chakrabarty, T., Kumar, M., Rajesh, K., Shahi, V. K., and Natarajan, T. (2010). Nanofibrous sulfonated poly (ether ether ketone) membrane for selective electro-transport of ions. Sep. Purif. Technol. 75, 174–182. doi:10.1016/j.seppur.2010.07.019
- Chan, E. P., Frieberg, B. R., Ito, K., Tarver, J., Tyagi, M., Zhang, W., et al. (2020). Insights into the water transport mechanism in polymeric membranes from neutron scattering. *Macromolecules* 53, 1443–1450. doi:10.1021/acs.macromol.9b02195
- Chede, S., Griffiths, P., Escobar, I. C., and Harris, T. A. (2018). Does casting method matter in filtration membranes? A comparison in performance between doctor blade and slot-die extruded polymeric membranes. *J. Appl. Polym. Sci.* 135, 45563. doi:10.1002/app.45563
- Chen, X. C., Oh, H. J., Yu, J. F., Yang, J. K., Petzetakis, N., Patel, A. S., et al. (2016). Block copolymer membranes for efficient capture of a chemotherapy drug. *ACS macro Lett.* 5, 936–941. doi:10.1021/acsmacrolett.6b00459
- Chen, C.-C., Gorensek, M. B., Gourdon, C., Ndlela, S. C., Palou-Rivera, I., Scott, J. K., et al. (2020). "Special section: process intensification," in *Chemical engineering progress* (New York: American Institute of Chemical Engineers).
- Chen, N., Paek, S. Y., Lee, J. Y., Park, J. H., Lee, S. Y., and Lee, Y. M. (2021). Highperformance anion exchange membrane water electrolyzers with a current density of 7.68 A cm— 2 and a durability of 1000 hours. *Energy Environ. Sci.* 14, 6338–6348. doi:10. 1039/d1ee02642a
- Chen, J. H., Choo, Y. S. L., Wang, X. H., Liu, Y. J., Yue, X. B., Gao, X. L., et al. (2023). Effects of the crown ether cavity on the performance of anion exchange membranes. J. Colloid Interface Sci. 643, 62–72. doi:10.1016/j.jcis.2023.04.011
- Choi, S., Park, S., and Nho, Y. (2000). Electrochemical properties of polyethylene membrane modified with carboxylic acid group. *Radiat. Phys. Chem.* 57, 179–186. doi:10.1016/S0969-806X(99)00347-3
- Choi, K. J., Choi, J. H., Hwang, E. H., Rhee, Y. W., and Hwang, T. S. (2007). Preparation and characterization of heterogeneous anion exchange membrane for recovery of sulfate ion from waste water. *Polymer-Korea* 31, 247–254.
- D'amato, A. R., Schaub, N. J., Cardenas, J. M., Franz, E., Rende, D., Ziemba, A. M., et al. (2017). Evaluation of procedures to quantify solvent retention in electrospun fibers and facilitate solvent removal. *Fibers Polym.* 18, 483–492. doi:10.1007/s12221-017-1061-5
- Dammak, L., Fouilloux, J., Bdiri, M., Larchet, C., Renard, E., Baklouti, L., et al. (2021). A review on ion-exchange membrane fouling during the electrodialysis process in the food industry, part 1: types, effects, characterization methods, fouling mechanisms and interactions. *Membr.* (*Basel*) 11, 789. doi:10.3390/membranes11100789
- Daud, S., Jaafar, J., Norddin, M., Sudirman, R., Onuomo, O. J., Ismail, A. F., et al. (2022). A review on process design and bilayer electrolyte materials of bipolar membrane fuel cell. *Int. J. Energy Res.* 46, 11620–11639. doi:10.1002/er.8014
- Deboli, F., Van Der Bruggen, B., and Donten, M. L. (2022). A versatile chemistry platform for the fabrication of cost-effective hierarchical cation and anion exchange membranes. *Desalination* 535, 115794. doi:10.1016/j.desal.2022.115794
- Dekel, D. R., Amar, M., Willdorf, S., Kosa, M., Dhara, S., and Diesendruck, C. E. (2017). Effect of water on the stability of quaternary ammonium groups for anion exchange membrane fuel cell applications. *Chem. Mater.* 29, 4425–4431. doi:10.1021/acs.chemmater.7b00958
- Depuydt, S., and Van Der Bruggen, B. (2024). Green synthesis of cation exchange membranes: a review. *Membranes* 14, 23. doi:10.3390/membranes14010023
- Doan, T. N. L., Hoang, T. K. A., and Chen, P. (2015). Recent development of polymer membranes as separators for all-vanadium redox flow batteries. *RSC Adv.* 5, 72805–72815. doi:10.1039/C5RA05914C
- Domhoff, A., and Davis, E. M. (2020). Influence of casting substrate on bulk morphology and vanadium ion transport in ionomer nanocomposites. *J. Appl. Phys.* 127, 174701. doi:10.1063/1.5144204
- Eker, A., Giammattia, M., Houpt, P., Kumar, A., Montero, O., Shah, M., et al. (2002). Intelligent extruder for polymer compounding. *GE Glob. Res.* 1999-2002, 98.

El-Rehim, H. A., Hegazy, E. S. A., and Ali, A. (2000). Selective separation of some heavy metals by poly (vinyl alcohol)-grafted membranes. *J. Appl. Polym. Sci.* 76, 125–132. doi:10.1002/(SICI)1097-4628(20000411)76:2<125::AID-APP2>3.0.CO;2-I

- Espiritu, R., Golding, B. T., Scott, K., and Mamlouk, M. (2018). Degradation of radiation grafted anion exchange membranes tethered with different amine functional groups via removal of vinylbenzyl trimethylammonium hydroxide. *J. Power Sources* 375, 373–386. doi:10.1016/j.jpowsour.2017.07.074
- Fanova, A., Sotiropoulos, K., Radulescu, A., and Papagiannopoulos, A. (2024). Advances in small angle neutron scattering on polysaccharide materials. *Polymers* 16, 490. doi:10.3390/polym16040490
- Festarini, R. V., Pham, M.-H., Liu, X., and Barz, D. P. (2017). A sugar-template manufacturing method for microsystem ion-exchange membranes. *J. Micromechanics Microengineering* 27, 075011. doi:10.1088/1361-6439/aa736b
- Fischer, L., Hartmann, S. S., Maljusch, A., Daeschlein, C., Prymak, O., and Ulbricht, M. (2023). The influence of anion-exchange membrane nanostructure onto ion transport: adjusting membrane performance through fabrication conditions. *J. Membr. Sci.* 669, 121306. doi:10.1016/j.memsci.2022.121306
- Flory, P. J. (1953). Principles of polymer chemistry. Ithaca, NY: Cornell University
- Foo, Z. H., and Lienhard, J. H. (2025). Emerging membrane technologies for sustainable lithium extraction from brines and leachates: innovations, challenges, and industrial scalability. *Desalination* 598, 118411. doi:10.1016/j.desal.2024.118411
- Fried, J. R. (2014). *Polymer science and technology*. Englewood Cliffs (NJ): PTR Prentice Hall.
- Galizia, M., Benedetti, F. M., Paul, D. R., and Freeman, B. D. (2017). Monovalent and divalent ion sorption in a cation exchange membrane based on cross-linked poly (p-styrene sulfonate-co-divinylbenzene). *J. Membr. Sci.* 535, 132–142. doi:10.1016/j. memsci.2017.04.007
- Gao, X. L., Sun, L. X., Wu, H. Y., Zhu, Z. Y., Xiao, N., Chen, J. H., et al. (2020). Highly conductive fluorine-based anion exchange membranes with robust alkaline durability. *J. Mater. Chem. A* 8, 13065–13076. doi:10.1039/d0ta04350h
- Garcia-Gutierrez, P., Klenert, D., Marschinski, R., Tonini, D., and Saveyn, H. (2023). Environmental and socio-economic sustainability of waste lubricant oil management in the EU. Luxembourg: Publications Office of the European Union. doi:10.2760/7597
- Garmsiri, M., and Mortaheb, H. R. (2015). Enhancing performance of hybrid liquid membrane process supported by porous anionic exchange membranes for removal of cadmium from wastewater. *Chem. Eng. J.* 264, 241–250. doi:10.1016/j. cej.2014.11.061
- Gebel, G. (2000). Structural evolution of water swollen perfluorosulfonated ionomers from dry membrane to solution. *polymer* 41, 5829–5838. doi:10.1016/S0032-3861(99)
- Gebel, G., and Diat, O. (2005). Neutron and X-ray scattering: suitable tools for studying ionomer membranes. Fuel Cells 5, 261–276. doi:10.1002/fuce.200400080
- Geise, G. M., Lee, H. S., Miller, D. J., Freeman, B. D., Mcgrath, J. E., and Paul, D. R. (2010). Water purification by membranes: the role of polymer science. *J. Polym. Sci. Part B Polym. Phys.* 48, 1685–1718. doi:10.1002/polb.22037
- Geise, G. M., Park, H. B., Sagle, A. C., Freeman, B. D., and Mcgrath, J. E. (2011). Water permeability and water/salt selectivity tradeoff in polymers for desalination. *J. Membr. Sci.* 369, 130–138. doi:10.1016/j.memsci.2010.11.054
- Geise, G. M., Cassady, H. J., Paul, D. R., Logan, B. E., and Hickner, M. A. (2014a). Specific ion effects on membrane potential and the permselectivity of ion exchange membranes. *Phys. Chem. Chem. Phys.* 16, 21673–21681. doi:10.1039/c4cp03076a
- Geise, G. M., Paul, D. R., and Freeman, B. D. (2014b). Fundamental water and salt transport properties of polymeric materials. *Prog. Polym. Sci.* 39, 1–42. doi:10.1016/j. progpolymsci.2013.07.001
- Ghoussoub, Y. E., Fares, H. M., Delgado, J. D., Keller, L. R., and Schlenoff, J. B. (2018). Antifouling ion-exchange resins. ACS Appl. Mater. Interfaces 10, 41747–41756. doi:10. 1021/acsami.8b12865
- Gierke, T., and Hsu, W. (1982). The cluster—network model of ion clustering in perfluorosulfonated membranes. Washington, DC, United States: American Chemical Society.
- Giles, H. F., Mount Iii, E. M., and Wagner, J. R. (2004). Extrusion: the definitive processing guide and handbook. Waltham, MA: William Andrew.
- Gohil, G., Binsu, V., and Shahi, V. K. (2006). Preparation and characterization of mono-valent ion selective polypyrrole composite ion-exchange membranes. *J. Membr. Sci.* 280, 210–218. doi:10.1016/j.memsci.2006.01.020
- Gottesfeld, S., Dekel, D. R., Page, M., Bae, C., Yan, Y., Zelenay, P., et al. (2018). Anion exchange membrane fuel cells: current status and remaining challenges. *J. Power Sources* 375, 170–184. doi:10.1016/j.jpowsour.2017.08.010
- Gurreri, L., Tamburini, A., Cipollina, A., and Micale, G. (2020). Electrodialysis applications in wastewater treatment for environmental protection and resources recovery: a systematic review on progress and perspectives. *Membranes* 10, 146. doi:10.3390/membranes10070146

Hallinan, D. T. (2009). "Transport in polymer electrolyte membranes using timeresolved FTIR-ATR spectroscopy,". PhD Dissertation. Philadelphia (PA): Drexel University.

- Hallinan, D. T., and Balsara, N. P. (2013). Polymer electrolytes. *Annu. Rev. Mater. Res.* 43, 503–525. doi:10.1146/annurev-matsci-071312-121705
- Hallinan, D. T., and Elabd, Y. A. (2007). Diffusion and sorption of methanol and water in Nafion using time-resolved fourier transform infrared-attenuated total reflectance spectroscopy. *J. Phys. Chem. B* 111, 13221–13230. doi:10.1021/jp075178n
- Harris, T. A., and Walczyk, D. F. (2006). Development of a casting technique for membrane material used in high-temperature PEM fuel cells. *J. Manuf. Process.* 8, 8–20. doi:10.1016/S1526-6125(06)70097-4
- Hays, S. S., and Pokorski, J. K. (2025). Solvent-free membrane manufacturing via melt processing. *Curr. Opin. Chem. Eng.* 47, 101061. doi:10.1016/j.coche.2024.101061
- Helfferich, F. G. (1995). *Ion exchange*. Mineola (NY): McGraw-Hill Courier Corporation
- Henkensmeier, D., Najibah, M., Harms, C., Žitka, J., Hnát, J., and Bouzek, K. (2021). Overview: state-of-the art commercial membranes for anion exchange membrane water electrolysis. *J. Electrochem. Energy Convers. Storage* 18, 024001. doi:10.1115/1.4047963
- Hensley, J. E., and Way, J. D. (2007). The relationship between proton conductivity and water permeability in composite carboxylate/sulfonate perfluorinated ionomer membranes. *J. power sources* 172, 57–66. doi:10.1016/j.jpowsour.2006.12.014
- Hittorf, W. (1899). "On the migration of ions during electrolysis," in *The fundamental laws of electrolytic conduction*. Editor H. M. GOODWIN (New York and London: Harper and Brothers).
- Ho, W., and Sirkar, K. (2012). *Membrane handbook*. Springer Science and Business Media.
- Hori, Y., Nakatani, T., and Mizutani, Y. (1986). Morphology of ion exchange membranes. *Microscopy* 35, 220–226. doi:10.1093/oxfordjournals.jmicro.a050571
- Hosseini, S., Gholami, A., Madaeni, S., Moghadassi, A., and Hamidi, A. (2012). Fabrication of (polyvinyl chloride/cellulose acetate) electrodialysis heterogeneous cation exchange membrane: characterization and performance in desalination process. *Desalination* 306, 51–59. doi:10.1016/j.desal.2012.07.028
- Hsu, W. Y., and Gierke, T. D. (1983). Ion transport and clustering in Nafion perfluorinated membranes. *J. Membr. Sci.* 13, 307–326. doi:10.1016/S0376-7388(00) 81563-X
- Hu, C., Wang, Y., and Lee, Y. M. (2025). Ether-free alkaline polyelectrolytes for water electrolyzers: recent advances and perspectives. *Angew. Chem. Int. Ed.* 64, e202418324. doi:10.1002/anie.202418324
- Hyder, A. G., Nuraeni, B., Gallagher, S. M., Wasilk, M., Macholz, J. D., Lipson, A. L., et al. (2025). Lithium recovery and conversion from wastewater produced by recycling of Li-Ion batteries via two-stage electrodialysis. *ACS Sustain. Chem. Eng.* 13, 4651–4660. doi:10.1021/acssuschemeng.4c07708
- James, P., Mcmaster, T., Newton, J., and Miles, M. (2000). *In situ* rehydration of perfluorosulphonate ion-exchange membrane studied by AFM. *Polymer* 41, 4223–4231. doi:10.1016/S0032-3861(99)00641-2
- Jana, K. K., Lue, S. J., Huang, A., Soesanto, J. F., and Tung, K. L. (2018). Separator membranes for high energy-density batteries. *ChemBioEng Rev.* 5, 346–371. doi:10. 1002/cben.201800014
- Jaroszek, H., and Dydo, P. (2016). Ion-exchange membranes in chemical synthesis—a review. *Open Chem.* 14, 1–19. doi:10.1515/chem-2016-0002
- Jia, G. Y., Zhu, Z. F., Li, S. N., Lu, Y., and Zhu, Y. Q. (2019). Facile preparation of poly (2,6-dimethyl-1,4-phenylene oxide)-based anion exchange membranes with improved alkaline stability. *Int. J. Hydrogen Energy* 44, 11877–11886. doi:10.1016/j.ijhydene.2019.
- Jokela, K., Serimaa, R., Torkkeli, M., Sundholm, F., Kallio, T., and Sundholm, G. (2002). Effect of the initial matrix material on the structure of radiation-grafted ion-exchange membranes: wide-angle and small-angle x-ray scattering studies. *J. Polym. Sci. Part B Polym. Phys.* 40, 1539–1555. doi:10.1002/polb.10217
- Jun, M.-S., Choi, Y.-W., and Kim, J.-D. (2012). Solvent casting effects of sulfonated poly(ether ether ketone) for polymer electrolyte membrane fuel cell. *J. Membr. Sci.* 396, 32–37. doi:10.1016/j.memsci.2011.12.008
- Kakimoto, M.-A., Grunzinger, S. J., and Hayakawa, T. (2010). Hyperbranched poly (ether sulfone) s: preparation and application to ion-exchange membranes. *Polym. J.* 42, 697–705. doi:10.1038/pj.2010.70
- Kamcev, J., and Freeman, B. D. (2016). Charged polymer membranes for environmental/energy applications. *Annu. Rev. Chem. Biomol. Eng.* 7, 111–133. doi:10.1146/annurev-chembioeng-080615-033533
- Kang, G., Woo, Y., Kim, H., Rhee, J.-W., Cheong, S., and Jung, I. (2013). *Microporous polyolefin film and method for preparing the same*. Washington, DC, United States: U.S. Patent and Trademark Office.
- Karimi, A., Mirfarsi, S. H., Rowshanzamir, S., Beyraghi, F., and Lester, D. (2020). Vicious cycle during chemical degradation of sulfonated aromatic proton exchange

membranes in the fuel cell application. *Int. J. Energy Res.* 44, 8877–8891. doi:10.1002/er.

- Khan, M. I., Shanableh, A., Khraisheh, M., and Almomani, F. (2022). Synthesis of porous BPPO-based anion exchange membranes for acid recovery via diffusion dialysis. *Membranes* 12, 95. doi:10.3390/membranes12010095
- Khoiruddin, A., Subagjo, D., and Wenten, I. G. (2017). Surface modification of ion-exchange membranes: methods, characteristics, and performance. *J. Appl. Polym. Sci.* 134, 45540. doi:10.1002/app.45540
- Kim, Y., Shin, S.-H., Chang, I. S., and Moon, S.-H. (2014). Characterization of uncharged and sulfonated porous poly (vinylidene fluoride) membranes and their performance in microbial fuel cells. *J. Membr. Sci.* 463, 205–214. doi:10.1016/j.memsci. 2014.03.061
- Kim, J. H., Vinothkannan, M., Kim, A. R., and Yoo, D. J. (2020). Anion exchange membranes obtained from Poly(arylene ether sulfone) block copolymers comprising hydrophilic and hydrophobic segments. *Polymers* 12, 325. doi:10.3390/polym12020325
- Kim, K., Zervoudakis, A. J., Lanasa, J. A., Haugstad, G., Zhou, F., Lee, B., et al. (2023a). Polyethylene blends for improved oxygen barrier: processing-dependent microstructure and gas permeability. ACS Appl. Polym. Mater. 6, 524–533. doi:10.1021/acsapm.
- Kim, S., Alayande, A. B., Eisa, T., Jang, J., Kang, Y., Yang, E., et al. (2023b). Fabrication and performance evaluation of a cation exchange membrane using graphene oxide/polyethersulfone composite nanofibers. *Membranes* 13, 633. doi:10.3390/membranes13070633
- Kirlioglu, A. C., Mojarrad, N. R., Gürsel, S. A., Güler, E., and Kaplan, B. Y. (2024). New generation radiation-grafted PVDF-g-VBC based dual-fiber electrospun anion exchange membranes. *Int. J. Hydrogen Energy* 51, 1390–1401. doi:10.1016/j.ijhydene. 2023.05.345
- Kirsh, Y. E., Smirnov, S. A., Popkov, Y. M., and Timashev, S. F. (1990). Perfluorinated carbon-chain copolymers with functional groups and cation exchange membranes based on them: synthesis, structure and properties. *Russ. Chem. Rev.* 59, 560–574. doi:10.1070/RC1990v059n06ABEH003543
- Kitto, D., and Kamcev, J. (2023). The need for ion-exchange membranes with high charge densities. *J. Membr. Sci.* 677, 121608. doi:10.1016/j.memsci.2023.121608
- Kitto, D., and Kamcev, J. (2024). Predicting the conductivity–selectivity trade-off and upper bound in ion-exchange membranes. *ACS Energy Lett.* 9, 1346–1352. doi:10.1021/acsenergylett.4c00301
- Klaysom, C., Moon, S. H., Ladewig, B. P., Lu, G. Q. M., and Wang, L. Z. (2011). Preparation of porous ion-exchange membranes (IEMs) and their characterizations. *J. Membr. Sci.* 371, 37–44. doi:10.1016/j.memsci.2011.01.008
- Kojima, T., Takano, T., and Komiyama, T. (1995). Selective permeation of metal ions through cation exchange membrane carrying N-(8-quinolyl)-sulfonamide as a chelating ligand. *J. Membr. Sci.* 102, 49–54. doi:10.1016/0376-7388(94)00244-S
- Komkova, E., Stamatialis, D., Strathmann, H., and Wessling, M. (2004). Anion-exchange membranes containing diamines: preparation and stability in alkaline solution. *J. Membr. Sci.* 244, 25–34. doi:10.1016/j.memsci.2004.06.026
- Kovalev, N., Karpenko, T., Averyanov, I., Sheldeshov, N., and Zabolotsky, V. (2022). Bipolar membrane with phosphoric acid catalyst for dissociation of water molecules: preparation, electrochemical properties, and application. *Membr. Membr. Technol.* 4, 347–356. doi:10.1134/S2517751622050067
- Kruczek, B., and Matsuura, T. (2003). Effect of solvent on properties of solution-cast dense SPPO films. *J. Appl. Polym. Sci.* 88, 1100–1110. doi:10.1002/app.12032
- Kumari, M., Douglin, J. C., and Dekel, D. R. (2021). Crosslinked quaternary phosphonium-functionalized poly (ether ether ketone) polymer-based anion-exchange membranes. *J. Membr. Sci.* 626, 119167. doi:10.1016/j.memsci.2021. 119167
- Kusoglu, A., and Weber, A. Z. (2017). New insights into perfluorinated sulfonic-acid ionomers. *Chem. Rev.* 117, 987–1104. doi:10.1021/acs.chemrev.6b00159
- Kwon, S., and Lee, S. (2020). Accurate measurement of self-diffusion coefficient of nanoparticles in aqueous solutions using a dynamic light scattering. *J. Korean Phys. Soc.* 77, 700–706. doi:10.3938/jkps.77.700
- La Corte, D., Vassallo, F., Cipollina, A., Turek, M., Tamburini, A., and Micale, G. (2020). A novel ionic exchange membrane crystallizer to recover magnesium hydroxide from seawater and industrial brines. *Membranes* 10, 303. doi:10.3390/membranes10110303
- Lazanas, A. C., and Prodromidis, M. I. (2023). Electrochemical impedance spectroscopy— a tutorial. *ACS Meas. Sci.* 3, 162–193. doi:10.1021/acsmeasuresciau. 2c00070
- Lee, C. H., Vanhouten, D., Lane, O., Mcgrath, J. E., Hou, J., Madsen, L. A., et al. (2011). Disulfonated poly (arylene ether sulfone) random copolymer blends tuned for rapid water permeation via cation complexation with poly (ethylene glycol) oligomers. *Chem. Mater.* 23, 1039–1049. doi:10.1021/cm1032173
- Lenkiewicz, Z. (2024). "Global waste management outlook 2024," in *Beyond an age of waste: turning rubbish into a resource* (Nairobi, Quênia: United Nations Environment Programme). doi:10.59117/20.500.11822/44939

Leo, C. M., Alonzo, S. N., Grumbles, E., and Kennemur, J. G. (2024). Sulfonated aromatic polypentenamers: scope of the acetyl sulfate reaction. *Macromolecules* 57, 8610–8620. doi:10.1021/acs.macromol.4c01145

- Li, X., Zuo, P., Ge, X., Yang, Z., and Xu, T. (2025). Constructing new-generation ion exchange membranes under confinement regime. *Natl. Sci. Rev.* 12, nwae439. doi:10. 1093/nsr/nwae439
- Liao, J., Yu, X., Pan, N., Li, J., Shen, J., and Gao, C. (2019). Amphoteric ion-exchange membranes with superior mono-/bi-valent anion separation performance for electrodialysis applications. *J. Membr. Sci.* 577, 153–164. doi:10.1016/j.memsci.2019. 01.052
- Lin, H., Ramos, L., Hwang, J., Zhu, T., Hossain, M. W., Wang, Q., et al. (2023). Main-chain cobaltocenium-containing ionomers for alkaline anion-exchange membranes. *Macromolecules* 56, 6375–6384. doi:10.1021/acs.macromol.3c01384
- Lindenbaum, S., Boyd, G., and Myers, G. (1958). Properties of a new strong base anion exchanger containing structurally bound tertiary sulfonium cations. *J. Phys. Chem.* 62, 995–999. doi:10.1021/j150566a028
- Liu, T., Lei, L., Gu, J., Wang, Y., Winnubst, L., Chen, C., et al. (2017). Enhanced water desalination performance through hierarchically-structured ceramic membranes. *J. Eur. Ceram. Soc.* 37, 2431–2438. doi:10.1016/j.jeurceramsoc.2017.02.001
- Liu, L., Wang, C., He, Z. F., Das, R. A. J., Dong, B. B., Xie, X. F., et al. (2021). An overview of amphoteric ion exchange membranes for vanadium redox flow batteries. J. Mater. Sci. Technol. 69, 212–227. doi:10.1016/j.jmst.2020.08.032
- Luo, X., Lau, G., Tesfaye, M., Arthurs, C. R., Cordova, I., Wang, C., et al. (2021). Thickness dependence of proton-exchange-membrane properties. *J. Electrochem. Soc.* 168, 104517. doi:10.1149/1945-7111/ac2973
- Marino, M. G., and Kreuer, K. D. (2015). Alkaline stability of Quaternary ammonium cations for alkaline fuel cell membranes and ionic liquids. ChemSusChem~8, 513-523. doi:10.1002/cssc.201403022
- Mauritz, K. A., and Moore, R. B. (2004). State of understanding of Nafion. *Chem. Rev.* 104, 4535–4585. doi:10.1021/cr0207123
- Mazrou, S., Kerdjoudj, H., Che, A. T., Elmidaoui, A., and Mole, J. (1998). Regeneration of hydrochloric acid and sodium hydroxide with bipolar membrane electrodialysis from pure sodium chloride. *New J. Chem.* 22, 355–361. doi:10.1039/a708753e
- Mcnair, R., Cseri, L., Szekely, G., and Dryfe, R. (2020). Asymmetric membrane capacitive deionization using anion-exchange membranes based on quaternized polymer blends. *Acs Appl. Polym. Mater.* 2, 2946–2956. doi:10.1021/acsapm.0c00432
- Mei, X., Yang, S., Lu, P., Zhang, Y., and Zhang, J. (2020). Improving the selectivity of ZIF-8/Polysulfone-Mixed matrix membranes by polydopamine modification for H2/CO2 separation. *Front. Chem.* 8, 528. doi:10.3389/fchem.2020.00528
- Mizutani, Y. (1990). Structure of ion exchange membranes. J. Membr. Sci. 49, 121–144. doi:10.1016/S0376-7388(00)80784-X
- Mizutani, Y., and Ikeda, K. (1987). Role of reinforcing material in ion exchange membranes prepared by the paste method. *J. Appl. Polym. Sci.* 34, 847–852. doi:10.1002/
- Mizutani, Y., and Nishimura, M. (1970). Studies on ion-exchange membranes. XXXII. Heterogeneity in ion-exchange membranes. *J. Appl. Polym. Sci.* 14, 1847–1856. doi:10. 1002/app.1970.070140718
- Mokrini, A., and Huneault, M. A. (2006). Proton exchange membranes based on PVDF/SEBS blends. *J. power sources* 154, 51–58. doi:10.1016/j.jpowsour.2005.04.021
- Mokrini, A., Huneault, M. A., and Gerard, P. (2006). Partially fluorinated proton exchange membranes based on PVDF-SEBS blends compatibilized with methylmethacrylate block copolymers. *J. Membr. Sci.* 283, 74–83. doi:10.1016/j.memsci.2006.06.032
- Mokrini, A., Raymond, N., Theberge, K., Robitaille, L., Del Rio, C., Ojeda, M., et al. (2010). Properties of melt-extruded vs. solution-cast proton exchange membranes based on PFSA nanocomposites. *ECS Trans.* 33, 855–865. doi:10.1149/1.3484579
- Münchinger, A., and Kreuer, K.-D. (2019). Selective ion transport through hydrated cation and anion exchange membranes I. The effect of specific interactions. *J. Membr. Sci.* 592, 117372. doi:10.1016/j.memsci.2019.117372
- Muthukumar, M. (2023). *Physics of charged macromolecules*. Cambridge, New York, NY: Combridge University Press.
- Nagarale, R., Gohil, G., and Shahi, V. K. (2006). Recent developments on ion-exchange membranes and electro-membrane processes. *Adv. Colloid Interface Sci.* 119, 97–130. doi:10.1016/j.cis.2005.09.005
- Nam, J., Huang, Y., Agarwal, S., and Lannutti, J. (2008). Materials selection and residual solvent retention in biodegradable electrospun fibers. *J. Appl. Polym. Sci.* 107, 1547–1554. doi:10.1002/app.27063
- Newman, J., and Thomas-Alyea, K. E. (2004). Electrochemical systems. Hoboken, NJ: Wiley-Interscience.
- Nguyen, N., Blatt, M. P., Kim, K., Hallinan, D. T., and Kennemur, J. G. (2022). Investigating miscibility and lithium ion transport in blends of poly (ethylene oxide) with a polyanion containing precisely-spaced delocalized charges. *Polym. Chem.* 13, 4309–4323. doi:10.1039/d2py00605g

Nishimura, M., and Mizutani, Y. (1981). Correlation between structure and properties of cation-exchange membranes prepared by the paste method. *J. Appl. Electrochem.* 11, 165–171. doi:10.1007/BF00610976

- Noshay, A., and Robeson, L. M. (1976). SULFONATED POLYSULFONE. J. Appl. Polym. Sci. 20, 1885–1903. doi:10.1002/app.1976.070200717
- Oh, H. J. (2015). Sulfonated polysulfone desalination membranes by melt extrusion. Dissertation. Austin (TX): University of Texas at Austin.
- Oh, Y.-J., Chung, S.-H., and Lee, M.-S. (2004). Optimization of thickness uniformity in electrodeposition onto a patterned substrate. *Mater. Trans.* 45, 3005–3010. doi:10. 2320/matertrans.45.3005
- Oh, H. J., Freeman, B. D., Mcgrath, J. E., Lee, C. H., and Paul, D. R. (2014). Thermal analysis of disulfonated poly (arylene ether sulfone) plasticized with poly (ethylene glycol) for membrane formation. *Polymer* 55, 235–247. doi:10.1016/j.polymer.2013.11.041
- Oh, H. J., Mcgrath, J. E., and Paul, D. R. (2017a). Kinetics of poly (ethylene glycol) extraction into water from plasticized disulfonated poly (arylene ether sulfone) desalination membranes prepared by solvent-free melt processing. *J. Membr. Sci.* 524, 257–265. doi:10.1016/j.memsci.2016.11.036
- Oh, H. J., Park, J., Inceoglu, S., Villaluenga, I., Thelen, J. L., Jiang, X., et al. (2017b). Formation of disulfonated poly (arylene ether sulfone) thin film desalination membranes plasticized with poly (ethylene glycol) by solvent-free melt extrusion. *Polymer* 109, 106–114. doi:10.1016/j.polymer.2016.12.035
- Oh, H. J., Mcgrath, J. E., and Paul, D. R. (2018). Water and salt transport properties of disulfonated poly (arylene ether sulfone) desalination membranes formed by solvent-free melt extrusion. *J. Membr. Sci.* 546, 234–245. doi:10.1016/j.memsci.2017.
- Oh, H. J., Aboian, M. S., Yi, M. Y., Maslyn, J. A., Loo, W. S., Jiang, X., et al. (2019). 3D printed absorber for capturing chemotherapy drugs before they spread through the body. ACS Central Sci. 5, 419–427. doi:10.1021/acscentsci.8b00700
- Oren, Y., Korngold, E., Daltrophe, N., Messalem, R., Volkman, Y., Aronov, L., et al. (2010). Pilot studies on high recovery BWRO-EDR for near zero liquid discharge approach. *Desalination* 261, 321–330. doi:10.1016/j.desal.2010.06.010
- Oroujzadeh, M., Mehdipour-Ataei, S., and Esfandeh, M. (2015). New proton exchange membranes based on sulfonated Poly(Arylene ether sulfone) copolymers: effect of chain structure on methanol crossover. *Int. J. Polym. Mater. Polym. Biomaterials* 64, 279–286. doi:10.1080/00914037.2014.936600
- Panayotova, M., and Panayotov, V. (2021). "Application of membrane processes in mining and mineral processing," in E3S Web of Conferences Les Ulis, France: EDP Sciences. doi:10.1051/e3sconf/202128008016
- Parnian, M. J., Rowshanzamir, S., and Gashoul, F. (2017). Comprehensive investigation of physicochemical and electrochemical properties of sulfonated poly (ether ether ketone) membranes with different degrees of sulfonation for proton exchange membrane fuel cell applications. *Energy* 125, 614–628. doi:10.1016/j.energy.2017.02.143
- Parrondo, J., Arges, C. G., Niedzwiecki, M., Anderson, E. B., Ayers, K. E., and Ramani, V. (2014). Degradation of anion exchange membranes used for hydrogen production by ultrapure water electrolysis. *Rsc Adv.* 4, 9875–9879. doi:10.1039/c3ra46630b
- Paul, D. R. (1976). The solution-diffusion model for swollen membranes. Sep. Purif. Methods 5, 33–50, doi:10.1080/03602547608066047
- Paul, D. R. (2004). Reformulation of the solution-diffusion theory of reverse osmosis. J. Membr. Sci. 241, 371–386. doi:10.1016/j.memsci.2004.05.026
- Peron, J., Mani, A., Zhao, X., Edwards, D., Adachi, M., Soboleva, T., et al. (2010). Properties of Nafion® NR-211 membranes for PEMFCs. *J. Membr. Sci.* 356, 44–51. doi:10.1016/j.memsci.2010.03.025
- Pham, T. H., Olsson, J. S., and Jannasch, P. (2017). N-spirocyclic quaternary ammonium ionenes for anion-exchange membranes. *J. Am. Chem. Soc.* 139, 2888–2891. doi:10.1021/jacs.6b12944
- Polat, K., and Sen, M. (2017). Preparation and characterization of a thermoplastic proton-exchange system based on SEBS and polypropylene blends. *Express Polym. Lett.* 11, 209–218. doi:10.3144/expresspolymlett.2017.22
- Price, W. S. (1998). Pulsed-field gradient nuclear magnetic resonance as a tool for studying translational diffusion: part II. Experimental aspects. *Concepts Magnetic Reson. An Educ. J.* 10, 197–237. doi:10.1002/(SICI)1099-0534(1998)10:4<197::AID-CMR1>3.0.CO;2-S
- Ramon, G. Z., Feinberg, B. J., and Hoek, E. M. V. (2011). Membrane-based production of salinity-gradient power. *Energy and Environ. Sci.* 4, 4423–4434. doi:10.1039/C1EE01913A
- Ran, J., Wu, L., He, Y., Yang, Z., Wang, Y., Jiang, C., et al. (2017). Ion exchange membranes: new developments and applications. *J. Membr. Sci.* 522, 267–291. doi:10.1016/j.memsci.2016.09.033
- Rao, R. R., Pandey, A., Hegde, A. R., Kulkarni, V. I., Chincholi, C., Rao, V., et al. (2021). Metamorphosis of twin screw extruder-based granulation technology: applications focusing on its impact on conventional granulation technology. *AAPS PharmSciTech* 23, 24. doi:10.1208/s12249-021-02173-w
- Reyes-Aguilera, J. A., Villafaña-López, L., Rentería-Martínez, E. C., Anderson, S. M., and Jaime-Ferrer, J. S. (2021). Electrospinning of polyepychlorhydrin and

polyacrylonitrile anionic exchange membranes for reverse electrodialysis. *Membranes* 11, 717. doi:10.3390/membranes11090717

- Rosato, D. (1998). Profiles. Extruding plastics: a practical processing handbook. Springer.
- Ryoo, G. W., Park, S. H., Kwon, K. C., Kang, J. H., Jang, H. W., and Kwon, M. S. (2024). Towards high-performance and robust anion exchange membranes (AEMs) for water electrolysis: super-acid-catalyzed synthesis of AEMs. *J. Energy Chem.* 93, 478–510. doi:10.1016/j.jechem.2024.01.070
- Safronova, E. Y., Golubenko, D., Shevlyakova, N., D'yakova, M., Tverskoi, V., Dammak, L., et al. (2016). New cation-exchange membranes based on cross-linked sulfonated polystyrene and polyethylene for power generation systems. *J. Membr. Sci.* 515, 196–203. doi:10.1016/j.memsci.2016.05.006
- Sagle, A. C., Van Wagner, E. M., Ju, H., Mccloskey, B. D., Freeman, B. D., and Sharma, M. M. (2009). PEG-coated reverse osmosis membranes: desalination properties and fouling resistance. *J. Membr. Sci.* 340, 92–108. doi:10.1016/j.memsci.2009.05.013
- Sankar, S., Roby, S., Kuroki, H., Miyanishi, S., Tamaki, T., Anilkumar, G. M., et al. (2023). High-performing anion exchange membrane water electrolysis using self-supported metal phosphide anode catalysts and an ether-free aromatic polyelectrolyte. ACS Sustain. Chem. and Eng. 11, 854–865. doi:10.1021/acssuschemeng.2c03663
- Sarapulova, V., Nevakshenova, E., Nebavskaya, X., Kozmai, A., Aleshkina, D., Pourcelly, G., et al. (2018). Characterization of bulk and surface properties of anion-exchange membranes in initial stages of fouling by red wine. *J. Membr. Sci.* 559, 170–182. doi:10.1016/j.memsci.2018.04.047
- Sata, T., Yoshida, T., and Matsusaki, K. (1996). Transport properties of phosphonic acid and sulfonic acid cation exchange membranes. *J. Membr. Sci.* 120, 101–110. doi:10. 1016/0376-7388(96)00159-7
- Schlenoff, J. B. (2014). Zwitteration: coating surfaces with zwitterionic functionality to reduce nonspecific adsorption. *Langmuir* 30, 9625–9636. doi:10.1021/la500057j
- Selzer, R. B., and Howery, D. G. (1986). Phosphoric acid ester cation-exchange resins.

  1. Synthesis and preliminary characterization. *Macromolecules* 19, 2673–2679. doi:10.1021/ma00165a001
- Shah, M., Al Mesfer, M. K., and Nagar, H. (2024). Static and dynamic properties investigation of modified polyethersulfone membrane for direct methanol fuel cell applications. *J. Power Sources* 615, 235086. doi:10.1016/j.jpowsour.2024.235086
- Shahi, V. K., Thampy, S., and Rangarajan, R. (2000). Preparation and electrochemical characterization of sulfonated interpolymer of polyethylene and styrene–divinylbenzene copolymer membranes. *React. Funct. Polym.* 46, 39–47. doi:10.1016/S1381-5148(00) 00031-6
- Shaik, S., Kundu, J., Yuan, Y., Chung, W., Han, D., Lee, U., et al. (2024). Recent progress and perspective in pure water-fed anion exchange membrane water electrolyzers. *Adv. Energy Mater.* 14, 2401956. doi:10.1002/aenm.202401956
- Shang, L., Yao, D., Pang, B., and Zhao, C. (2021). Anion exchange membranes based on poly (ether ether ketone) containing N-spirocyclic quaternary ammonium cations in phenyl side chain. *Int. J. Hydrogen Energy* 46, 19116–19128. doi:10.1016/j.ijhydene. 2021.03.059
- Sharkh, B. A., Al-Amoudi, A. A., Farooque, M., Fellows, C. M., Ihm, S., Lee, S., et al. (2022). Seawater desalination concentrate—a new frontier for sustainable mining of valuable minerals. *Npj Clean. Water* 5, 9. doi:10.1038/s41545-022-00153-6
- Siemann, U. (2005). "Solvent cast technology-a versatile tool for thin film production," in Scattering methods and the properties of polymer materials. Springer.
- Sim, J., Lee, J., Rho, H., Park, K.-D., Choi, Y., Kim, D., et al. (2023). A review of semiconductor wastewater treatment processes: current status, challenges, and future trends. *J. Clean. Prod.* 429, 139570. doi:10.1016/j.jclepro.2023.139570
- Simari, C., Lufrano, E., Corrente, G. A., and Nicotera, I. (2021). Anisotropic behavior of mechanically extruded sulfonated polysulfone: implications for proton exchange membrane fuel cell applications. *Solid State Ionics* 362, 115581. doi:10.1016/j.ssi.2021. 115581
- Slade, S., Ralph, T., Ponce De León, C., Campbell, S. A., and Walsh, F. C. (2010). The ionic conductivity of a nafion  $^{\circ}$  1100 series of proton-exchange membranes re-cast from Butan-1-ol and Propan-2-ol. *Fuel Cells* 10, 567–574. doi:10.1002/fuce.200900118
- Soni, R., Miyanishi, S., Kuroki, H., and Yamaguchi, T. (2020). Pure water solid alkaline water electrolyzer using fully aromatic and high-molecular-weight poly (fluorene-alt-tetrafluorophenylene)-trimethyl ammonium anion exchange membranes and ionomers. ACS Appl. Energy Mater. 4, 1053–1058. doi:10.1021/acsaem.0c01938
- Stránská, E., Weinertová, K., Nedela, D., and Krivcík, J. (2018). Preparation and basic characterization of heterogeneous weak acid cation exchange membrane. *Chem. Pap.* 72, 89–98. doi:10.1007/s11696-017-0260-2
- Su, Y.-N., Lin, W.-S., Hou, C.-H., and Den, W. (2014). Performance of integrated membrane filtration and electrodialysis processes for copper recovery from wafer polishing wastewater. *J. Water Process Eng.* 4, 149–158. doi:10.1016/j.jwpe.2014.09.012
- Su, G. M., Cordova, I. A., and Wang, C. (2020). New insights into water treatment materials with chemically sensitive soft and tender X-rays. *Synchrotron Radiat. News* 33, 17–23. doi:10.1080/08940886.2020.1784695

Sudoh, M., Kamei, H., Nakamura, S., and Kawamori, M. (1990a). Donnan dialysis concentration using cation exchange membrane prepared by paste method. *J. Chem. Eng. Jpn.* 23, 680–685. doi:10.1252/jcej.23.680

- Sudoh, M., Kawamori, M., Minamoto, K., and Anzai, K. (1990b). Effect of intramembrane structure on transport properties of cation exchange membrane prepared by paste method. *J. Chem. Eng. Jpn.* 23, 728–734. doi:10.1252/jcej.23.728
- Swaby, S., Ureña, N., Pérez-Prior, M. T., Del Río, C., Várez, A., Sanchez, J. Y., et al. (2023). Proton conducting sulfonated polysulfone and polyphenylsulfone multiblock copolymers with improved performances for fuel cell applications. *J. Industrial Eng. Chem.* 122, 366–377. doi:10.1016/j.jiec.2023.02.037
- Tanaka, N., Nagase, M., and Higa, M. (2010). Organic fouling behavior of anion exchange membranes prepared from chloromethyl styrene and divinylbenzene. *Desalination water Treat.* 17, 248–254. doi:10.5004/dwt.2010.1725
- Tanaka, N., Nagase, M., and Higa, M. (2011). Preparation of aliphatic-hydrocarbon-based anion-exchange membranes and their anti-organic-fouling properties. *J. Membr. Sci.* 384, 27–36. doi:10.1016/j.memsci.2011.08.064
- Tang, W., Zhang, R., Liu, B., and Yuan, H. (2014). Perfluorosulfonated ionomers membranes: melt-processing and characterization for ion exchange applications. *J. Appl. Polym. Sci.* 131, app.39944. doi:10.1002/app.39944
- Tsou, A., Hord, J., Smith, G., and Schrader, R. (1992). Strength analysis of polymeric films. *Polymer* 33, 2970–2974. doi:10.1016/0032-3861(92)90083-9
- Vahedi, N., Nourmohammadi, J., and Jalili, H. (2024). Nanocomposite membrane of alumina nanofibers/poly ether sulfone as blood-contacting biomaterials. *Mater. Today Commun.* 39, 109145, doi:10.1016/j.mtcomm.2024.109145
- Vasylkevych, O., and Slisenko, V. (2019). "Self-diffusion of molecules in water-ethanol solutions of low concentration," in *Neutron data*. Ukraine: Publishing House "Akademperiodyka" National Academy of Sciences of Ukraine) 46–51. doi:10.15407/dopovidi2019.08.046
- Venkatachalam, K. R., Gautham, S. M. B., and Krishnan, J. N. N. (2023). Desalination characteristics of new blend membranes based on sulfonated polybenzimidazole and sulfonated poly(arylene ether sulfone). *Polym. Bull.* 80, 7805–7824. doi:10.1007/s00289-022-04428-3
- Vijayakrishna, K., Jewrajka, S. K., Ruiz, A., Marcilla, R., Pomposo, J. A., Mecerreyes, D., et al. (2008). Synthesis by RAFT and ionic responsiveness of double hydrophilic block copolymers based on ionic liquid monomer units. *Macromolecules* 41, 6299–6308. doi:10.1021/ma800677h
- Vlachopoulos, J., and Polychronopoulos, N. D. (2019). *Understanding rheology and technology of polymer extrusion*. Dundas, ON, Canada: Polydynamics Inc.
- Vogel, B., Dilger, H., and Roduner, E. (2010). Rapid radical degradation test of polyaromatic fuel cell membranes by electron paramagnetic resonance. *Macromolecules* 43, 4688–4697. doi:10.1021/ma1006073
- Voigt, U., Khrenov, V., Tauer, K., Hahn, M., Jaeger, W., and Von Klitzing, R. (2002). The effect of polymer charge density and charge distribution on the formation ofmultilayers. *J. Phys. Condens. Matter* 15, S213–S218. doi:10.1088/0953-8984/15/1/327
- Wamble, N. P., Eugene, E. A., Phillip, W. A., and Dowling, A. W. (2022). Optimal diafiltration membrane cascades enable green recycling of spent lithium-ion batteries. *ACS Sustain. Chem. Eng.* 10, 12207–12225. doi:10.1021/acssuschemeng.2c02862
- Wang, Y., Zhang, Z., Jiang, C., and Xu, T. (2013). Electrodialysis process for the recycling and concentrating of tetramethylammonium hydroxide (TMAH) from photoresist developer wastewater. *Industrial Eng. Chem. Res.* 52, 18356–18361. doi:10.1021/ie4023995
- Wang, C., Feng, Z., Zhao, Y., Li, X., Li, W., Xie, X., et al. (2017). Preparation and properties of ion exchange membranes for PEMFC with sulfonic and carboxylic acid groups based on polynorbornenes. *Int. J. Hydrogen Energy* 42, 29988–29994. doi:10. 1016/j.ijhydene.2017.09.168
- Wang, Y., Yang, Z., Wu, L., Ge, L., and Xu, T. (2021). Ion exchange membrane "ABC"–A key material for upgrading process industries. *Chin. J. Chem.* 39, 825–837. doi:10.1002/cjoc.202000473
- Werber, J. R., Deshmukh, A., and Elimelech, M. (2016a). The critical need for increased selectivity, not increased water permeability, for desalination membranes. *Environ. Sci. Technol. Lett.* 3, 112–120. doi:10.1021/acs.estlett.6b00050
- Werber, J. R., Osuji, C. O., and Elimelech, M. (2016b). Materials for next-generation desalination and water purification membranes. *Nat. Rev. Mater.* 1, 16018. doi:10.1038/natrevmats.2016.18
- Wiley, R. H., and Reed, S. (1956). Sulfostyrenes. 1 polymers and copolymers of potassium p-Vinylbenzenesulfonate. *J. Am. Chem. Soc.* 78, 2171–2173. doi:10.1021/ja01591a041
- Wu, L., Zhao, Y., Ge, L., Yang, Z. J., Jiang, C. X., and Xu, T. W. (2015). One-pot preparation of anion exchange membranes from bromomethylated poly(2,6-dimethyl-1,4-phenylene oxide) for electrodialysis. *Chem. Eng. Sci.* 135, 526–531. doi:10.1016/j.ces. 2014.09.028
- Xie, W., Park, H.-B., Cook, J., Lee, C. H., Byun, G., Freeman, B. D., et al. (2010). Advances in membrane materials: desalination membranes based on directly copolymerized disulfonated poly (arylene ether sulfone) random copolymers. *Water Sci. Technol.* 61, 619–624. doi:10.2166/wst.2010.883

Xie, W., Geise, G. M., Freeman, B. D., Lee, C. H., and Mcgrath, J. E. (2012). Influence of processing history on water and salt transport properties of disulfonated polysulfone random copolymers. *Polymer* 53, 1581–1592. doi:10.1016/j.polymer.2012.01.046

- Xu, T. (2005). Ion exchange membranes: state of their development and perspective. *J. Membr. Sci.* 263, 1–29. doi:10.1016/j.memsci.2005.05.002
- Xu, X., Lin, L., Ma, G., Wang, H., Jiang, W., He, Q., et al. (2018). Study of polyethyleneimine coating on membrane permselectivity and desalination performance during pilot-scale electrodialysis of reverse osmosis concentrate. Sep. Purif. Technol. 207, 396–405. doi:10.1016/j.seppur.2018.06.070
- Xue, T., Trent, J., and Osseo-Asare, K. (1989). Characterization of nafion® membranes by transmission electron microscopy. *J. Membr. Sci.* 45, 261–271. doi:10.1016/S0376-7388(00)80518-9
- Yang, S. F., Gong, C. L., Guan, R., Zou, H., and Dai, H. (2006). Sulfonated poly(phenylene oxide) membranes as promising materials for new proton exchange membranes. *Polym. Adv. Technol.* 17, 360–365. doi:10.1002/pat.718
- Yang, J. S., Li, Q. F., Jensen, J. O., Pan, C., Cleemann, L. N., Bjerrum, N. J., et al. (2012). Phosphoric acid doped imidazolium polysulfone membranes for high temperature proton exchange membrane fuel cells. *J. Power Sources* 205, 114–121. doi:10.1016/j. jpowsour.2012.01.038
- Yang, J. S., Liu, C., Hao, Y. N., He, X. N., and He, R. H. (2016). Preparation and investigation of various imidazolium-functionalized poly(2,6-dimethyl-1,4-phenylene oxide) anion exchange membranes. *Electrochimica Acta* 207, 112–119. doi:10.1016/j. electacta.2016.04.176
- Yang, Q., Sun, L., Gao, W., Zhu, Z., Gao, X., Zhang, Q., et al. (2021). Crown ether-based anion exchange membranes with highly efficient dual ion conducting pathways. *J. Colloid Interface Sci.* 604, 492–499. doi:10.1016/j.jcis.2021.07.043
- Yang, P.-X., Wang, J., Liu, H.-L., Guo, Z.-Y., Huang, Z.-H., Zhang, P.-P., et al. (2024). High-performance monovalent selective cation exchange membranes with ionically cross-linkable side chains: effect of the acidic groups. ACS Appl. Mater. Interfaces 16, 35576–35587. doi:10.1021/acsami.4c07085
- Yang, Y., Bi, S., Wang, F., Pan, X., Yang, T., Hu, S., et al. (2025). Solid membrane-based aqueous lithium extraction and adsorption: advances, challenges, and prospects. *Chem. Eng. J.* 510, 161748. doi:10.1016/j.cej.2025.161748

- Yao, Q., and Wilkie, C. A. (1999). Thermal degradation of blends of polystyrene and poly (sodium 4-styrenesulfonate) and the copolymer, poly (styrene-co-sodium 4-styrenesulfonate). *Polym. Degrad. Stab.* 66, 379–384. doi:10.1016/S0141-3910(99) 00090-7
- Ye, Y., Stokes, K. K., Beyer, F. L., and Elabd, Y. A. (2013). Development of phosphonium-based bicarbonate anion exchange polymer membranes. *J. Membr. Sci.* 443, 93–99. doi:10.1016/j.memsci.2013.04.053
- Yeager, H., Twardowski, Z., and Clarke, L. (1982). A comparison of perfluorinated carboxylate and sulfonate ion exchange polymers: I. diffusion and water sorption. *J. Electrochem. Soc.* 129, 324–327. doi:10.1149/1.2123820
- Yee, R. S.-L., Rozendal, R. A., Zhang, K., and Ladewig, B. P. (2012). Cost effective cation exchange membranes: a review. *Chem. Eng. Res. Des.* 90, 950–959. doi:10.1016/j. cherd.2011.10.015
- Yee, R. S., Zhang, K., and Ladewig, B. P. (2013). The effects of sulfonated poly (ether ether ketone) ion exchange preparation conditions on membrane properties. *Membranes* 3, 182–195. doi:10.3390/membranes3030182
- Ying, J., Lin, Y., Zhang, Y., and Yu, J. (2023). Developmental progress of electrodialysis technologies and membrane materials for extraction of lithium from salt Lake brines. ACS ES&T Water 3, 1720–1739. doi:10.1021/acsestwater. 3c00013
- Zhang, M., Kim, H. K., Chalkova, E., Mark, F., Lvov, S. N., and Chung, T. M. (2011). New polyethylene based anion exchange membranes (PE-AEMs) with high ionic conductivity. *Macromolecules* 44, 5937–5946. doi:10.1021/ma200836d
- Zhao, C., Xue, J., Ran, F., and Sun, S. (2013). Modification of polyethersulfone membranes—A review of methods. *Prog. Mater. Sci.* 58, 76–150. doi:10.1016/j.pmatsci. 2012.07.002
- Zhong, W., Liu, F., and Wang, C. (2021). Probing morphology and chemistry in complex soft materials with *in situ* resonant soft x-ray scattering. *J. Phys. Condens. Matter* 33, 313001. doi:10.1088/1361-648X/ac0194
- Zulkifli, M. Z. A., Nordin, D., Shaari, N., and Kamarudin, S. K. (2023). Overview of electrospinning for tissue engineering applications. *Polymers* 15, 2418. doi:10.3390/polym15112418

# Glossary

EDL

LDPE

PAN

PE

PECH

SLM AEM anion-exchange membrane supported liquid membrane **AFM** atomic force microscopy SME specific mechanical energy

BPED bipolar membrane electrodialysis sPEEK sulfonated poly(ether ether ketone)

BPS disulfonated poly(arylene ether sulfone) sPIM sulfonated polymers of intrinsic microporosity

CE counter electrode sPS sulfonated polystyrene

CEM cation-exchange membrane sPS-DVB sulfonated polystyrene-divinylbenzene

Cu-CMP copper chemical mechanical planarization sPSf sulfonated polysulfone DLS dynamic light scattering SSE single-screw extruder DMA dynamic mechanical analysis St-DVB styrene-divinyl benzene

DMAc dimethylacetamide T-die T-shaped die

DS degree of sulfonation TEM transmission electron microscopy

DSC differential scanning calorimetry TGA thermogravimetric analysis

ED electrodialysis TMAH tetramethylammonium hydroxide

TSE

WE

twin-screw extruder

working electrode

electric double layer EIS electrochemical impedance spectroscopy UF ultrafiltration

universal testing machine FO forward osmosis UTM

IEC ion-exchange capacity WAXS wide-angle x-ray scattering

IEMC ion-exchange membrane crystallization WC water content

MFC microbial fuel cell ZwIEM zwitterionic ion-exchange membrane

NIPS non-solvent induced phase separation

NMR nuclear magnetic resonance

PEEK poly(ether ether ketone) PEG poly(ethylene glycol)

PEK poly(ether ketone) PES poly(ether sulfone)

**PFAP** poly(fluorenyl-co-aryl piperidinium)

low density polyethylene

polyacrylonitrile

polyepichlorohydrin

polyethylene

PFSA perfluorosulfonic acid

PIMs polymers of intrinsic microporosity

**PSf** polysulfone

PVC polyvinylchloride

**PVDF** poly(vinylidene fluoride)

QENS quasi-elastic neutron scattering

Ref reference electrode RO reverse osmosis

SANS small-angle neutron scattering small-angle x-ray scattering SAXS

SEBS styrene-(ethylene-butylene)-styrene